

---

# Counterfactual Analysis in Dynamic Latent State Models

---

Martin Haugh<sup>1</sup> Raghav Singal<sup>2</sup>

## Abstract

We provide an optimization-based framework to perform counterfactual analysis in a dynamic model with hidden states. Our framework is grounded in the “abduction, action, and prediction” approach to answer counterfactual queries and handles two key challenges where (1) the states are *hidden* and (2) the model is *dynamic*. Recognizing the lack of knowledge on the underlying causal mechanism and the possibility of infinitely many such mechanisms, we optimize over this space and compute upper and lower bounds on the counterfactual quantity of interest. Our work brings together ideas from causality, state-space models, simulation, and optimization, and we apply it on a breast cancer case study. To the best of our knowledge, we are the first to compute lower and upper bounds on a counterfactual query in a dynamic latent-state model.

## 1. Introduction

*Counterfactual analysis*, falling on the third rung of Pearl’s ladder of causation (Pearl & Mackenzie, 2018), is a fundamental problem in causality. It requires us to *imagine* a world where a certain policy was enacted with a corresponding outcome *given* that a different policy and outcome were actually observed. It is performed via the 3-step framework of *abduction* (conditioning on the observed data), *action* (changing the policy), and *prediction* (computing the counterfactual quantity of interest (CQI)), and has wide-ranging applications (Pearl, 2009a;b).

As a concrete application in healthcare and legal reasoning, consider someone who recently died from breast cancer. The exact progression of her disease is unknown. What is known, however, is that over a period of time prior to her diagnosis, her insurance company adopted a strategy of denying her regular scans (e.g., mammograms) even though these scans should have been covered by her policy. Had these scans gone ahead, the cancer may have been found

earlier and the patient’s life saved. Now a court wants to know the probability that her life would have been saved had the routine scans been permitted.

On top of the challenges posed by standard counterfactual analysis, there are two that are particular to such a setting. First, it is possible that the underlying state of the patient (e.g., stage of cancer) is *hidden / latent* and we only observe a noisy signal depending on the accuracy of the scan (e.g., sensitivity and specificity of a mammogram). Second, the underlying model is *dynamic* as the patient’s state evolves over time. As such, our goal in this work is to perform counterfactual analysis in dynamic latent state models.

Two streams of work are closely related to ours. The first relates to works on constructing bounds on CQIs (Balke & Pearl, 1994; Tian & Pearl, 2000; Kaufman et al., 2005; Cai et al., 2008; Pearl, 2009b; Mueller et al., 2021; Zhang et al., 2021). These papers focus on *static* models and generally consider binary variables. The second stream is more recent and concerns counterfactual analysis in dynamic models (Buesing et al., 2019; Oberst & Sontag, 2019; Lorberbom et al., 2021; Tsirtsis et al., 2021). Except Buesing et al. (2019), none of these works allows for *latent* states. In addition, these works perform counterfactual analysis by embedding assumptions strong enough that restrict the underlying set of causal mechanisms to a singleton. In particular, Buesing et al. (2019) explicitly fix a single causal mechanism whereas Oberst & Sontag (2019) and Tsirtsis et al. (2021) invoke *counterfactual stability* and implicitly fix the causal mechanism (via the Gumbel-max distribution). Lorberbom et al. (2021) extend the Gumbel-max approach but their choice of causal mechanism is the one that minimizes variance when estimating the CQI. In summary, none of these approaches explicitly account for all possible causal mechanisms, and therefore, they do not consider the construction of lower and upper bounds on the CQI, which is our focus.

Our key contribution is to provide a principled framework for counterfactual analysis in dynamic latent state models. We define our problem in §2 and discuss counterfactual stability in §3. In §4, we present our solution approach and we describe our numerics in §5. We conclude in §6.

---

<sup>1</sup>Imperial College <sup>2</sup>Dartmouth College. Correspondence to: MH <m.haugh@imperial.ac.uk>, RS <singal@dartmouth.edu>.

## 2. Problem Definition

We first define the underlying dynamic latent state model (§2.1) and then, the counterfactual analysis problem (§2.2). We will use the breast cancer application as a vehicle for explaining ideas throughout but it should be clear our framework is quite general.

### 2.1. A Dynamic Latent State Model

The model, visualized in Figure 1, has  $T$  discrete time periods. In each period  $t$ , the system is in a hidden state  $H_t \in \mathbb{H}$  (finite). As a stochastic function of  $H_t$  and the underlying policy  $X_t \in \mathbb{X}$  (finite), we observe an emission  $O_t \in \mathbb{O}$  (finite). The *emission probability* is denoted by  $e_{hxi} := \mathbb{P}(O_t = i \mid H_t = h, X_t = x)$  for all  $(h, x, i)$ . This is followed by the state  $H_t$  transitioning to  $H_{t+1}$  with *transition probability*  $q_{hh'}$  :=  $\mathbb{P}(H_{t+1} = h' \mid H_t = h, O_t = i)$ . The model  $\mathbf{M}$  comprises of three primitives:  $\mathbf{M} \equiv (\mathbf{p}, \mathbf{E}, \mathbf{Q})$ , where  $\mathbf{p} := [p_h]_h$  denotes the *initial state distribution* with  $p_h := \mathbb{P}(H_1 = h)$  for all  $h$ ,  $\mathbf{E} := [e_{hxi}]_{h,x,i}$ , and  $\mathbf{Q} := [q_{hh'}]_{h,i,h'}$ .

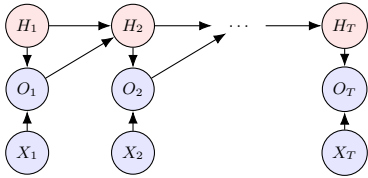


Figure 1. A dynamic latent state model. States  $H_{1:T}$  are hidden (red). Emissions  $O_{1:T}$  are observed (blue).  $X_{1:T}$  represents the policy (observed). (We use the notation  $X_{1:T} := (X_t)_{t=1}^T$ .)

For the breast cancer application, such a model has been used in academic research (Ayer et al., 2012; Haugh & Lacedelli, 2019) and its practical justification comes from the simulation model used by the National Cancer Institute (UWBCS, 2013). The time periods map to the frequency of mammograms (e.g., 6 months) and the hidden state  $H_t \in \{1, \dots, 7\}$  denotes the patient’s condition. State 1 equates to the patient being healthy whereas states 2 and 3 to *undiagnosed* in-situ and invasive breast cancer, respectively. States 4 and 5 correspond to *diagnosed* in-situ and invasive breast cancer respectively, with the understanding that the cancer treatment has begun (since it has been diagnosed). States 6 and 7 are absorbing and denote recovery from cancer (due to treatment) and death from cancer, respectively. The observation  $O_t \in \{1, \dots, 7\}$  captures the mammogram result. A value of 1 means no screening took place, whereas 2 denotes a negative screening result (possibly a false negative). A value of 3 corresponds to a positive mammogram result, but followed by a negative biopsy (i.e., the patient is healthy and the mammogram produced a false positive). Observations 4 and 5 map to correctly diagnosed in-situ and invasive cancer respectively, i.e., a positive mam-

mogram followed by a positive biopsy. Observations 6 and 7 are used to denote patient recovery and death from breast cancer, respectively. The variable  $X_t \in \{0, 1\}$  models the insurance company’s coverage policy for the mammograms, with 0 denoting the company covers it and 1 denoting the company (incorrectly) denies the coverage. If the coverage is denied, then the mammogram is not performed and hence, the observation cannot be 2, 3, 4, or 5. (In this application, the  $X_t$ ’s are deterministic but in general, they could be the result of a randomized policy.)

**Remark 1.** *Our model is a generalization of a hidden Markov model (HMM) since  $H_{t+1}$  depends not only on  $H_t$  but also  $O_t$ . In the breast cancer application, the dependence on  $O_t$  is needed to capture the fact that if cancer was detected during period  $t$  and treatment began at that point of time, i.e.,  $O_t \in \{4, 5\}$ , then  $H_{t+1}$  depends on the fact that the treatment began in period  $t$ . For example, if  $H_t = 2$  (in-situ cancer) and  $O_t = 4$  (in-situ diagnosed and hence, treatment began), then  $H_{t+1}$  would be different compared to when  $H_t = 2$  and  $O_t = 2$  (false negative and hence, treatment did not begin).*

### 2.2. The Counterfactual Analysis Problem

We now use our dynamic model to state the counterfactual analysis problem. We do so via two modules: (1) observed data and (2) counterfactual quantity of interest (CQI).

**Observed data.** Suppose we observe emissions  $o_{1:T}$  with the underlying policy being  $x_{1:T}$ . The true hidden states  $h_{1:T}$  are not observed. In the context of breast cancer, the observations for a particular patient might be as follows:

$$\underbrace{o_1, \dots, o_{\tau_s-1}}_{\in \{2,3\}}, \underbrace{o_{\tau_s}, \dots, o_{\tau_e}}_{=1}, \underbrace{o_{\tau_e+1}, \dots, o_{\tau_d-1}}_{\in \{4,5\}}, \underbrace{o_{\tau_d:T}}_{=7}. \quad (1)$$

That is, the patient was screened ( $x_{1:\tau_s-1} = 0$ ) and appeared healthy ( $o_{1:\tau_s-1} \in \{2, 3\}$ ) up to (and including) time  $\tau_s - 1$ . Coverage was then denied during periods  $\tau_s$  to  $\tau_e$  (i.e.,  $x_{\tau_s:\tau_e} = 1$ ; red font). Hence, screening was not performed during those periods ( $o_{\tau_s:\tau_e} = 1$ ). As soon as the coverage for screening was re-approved (period  $\tau_e + 1$  and hence,  $x_{\tau_e+1} = 0$ ), the patient was found to have cancer (either in-situ or invasive) and the corresponding treatment began; thus,  $o_{\tau_e+1} \in \{4, 5\}$ . Unfortunately, the patient died at  $\tau_d$ .

**CQI.** We focus on the well-known CQI of the *probability of necessity* (PN) (Pearl, 2009a), i.e., the probability the patient would have not died (counterfactual state  $\tilde{H}_T \neq 7$ ) had the screening been covered in every period (intervention policy  $\tilde{x}_{1:T} = 0$ ) given the observed data ( $o_{1:T}, x_{1:T}$ ). (We use “tilde” notation to denote quantities in the counterfactual world.) The interpretation of  $\tilde{x}_{1:T}$  is straightforward as it is fixed exogenously. However, the counterfactual state  $\tilde{H}_T$  is

obtained via the 3-step framework of abduction, action, and prediction (Pearl, 2009b). Step 1 (abduction) involves conditioning on the observed data  $(o_{1:T}, x_{1:T})$  to form a posterior belief over the hidden states. Step 2 (action) changes the policy from  $x_{1:T}$  to  $\tilde{x}_{1:T}$  and brings us to the counterfactual world  $\tilde{\mathbf{M}}$ . Finally, step 3 (prediction) computes PN in the counterfactual model:

$$\text{PN} = \mathbb{P}(\tilde{H}_T \neq 7), \quad (2)$$

with the understanding that the event  $\{\tilde{H}_T \neq 7\}$  is conditional on  $(o_{1:T}, x_{1:T})$ . Though we focus on PN, it is easy to extend our framework to a broad class of CQIs as the abduction and action steps do not depend on the CQI.

Given our focus on counterfactual analysis, we assume the primitives  $(\mathbf{p}, \mathbf{E}, \mathbf{Q})$  to be known. We discuss their calibration to real-world data in §5 and emphasize that even with known  $(\mathbf{p}, \mathbf{E}, \mathbf{Q})$ , counterfactual analysis is challenging. This is because we are interested in counterfactuals at an *individual* level (i.e., conditioning on the patient-level data  $(o_{1:T}, x_{1:T})$  via abduction), as opposed to the *population* level. A population-level counterfactual analysis would ignore the first step of abduction but simply change the policy to  $\tilde{x}_{1:T}$  to predict the CQI (by simulating the resulting model and obtaining a Monte-Carlo estimate of PN or doing it in closed-form if analytically tractable). However, this is very different from the task at hand, which falls on the highest rung of Pearl’s ladder of causation (Pearl & Mackenzie, 2018). For instance, consider a patient who dies right after the coverage was denied versus a patient who dies a couple of years after the coverage was denied. Clearly, the first patient had a more “aggressive” cancer and hence, we expect that her PN would be lower. By conditioning on individual-level data  $(o_{1:T}, x_{1:T})$ , we are able to account for such differences. However, it makes the problem much more challenging.

In our dynamic latent state model, each of the three steps of abduction, action, and prediction presents its own set of challenges<sup>1</sup>, which we discuss when presenting our methodology in §4. Before doing so, we discuss the notion of counterfactual stability, which has become a popular approach in such settings (Oberst & Sontag, 2019).

### 3. Limitations of Counterfactual Stability (CS)

Instead of discussing CS in our dynamic latent state model, we do so using the simple model of Figure 2. Suppose we observe an outcome  $Y = y$  under policy  $X = x$ . With  $Y_x := Y \mid (X = x)$ , CS requires that the counterfac-

tual outcome under an interventional policy  $\tilde{x}$  (denoted by  $\tilde{Y} := Y_{\tilde{x}} \mid Y_x = y$ ) can not be  $y'$  (for  $y' \neq y$ ) if  $\mathbb{P}(Y_{\tilde{x}} = y) / \mathbb{P}(Y_x = y) \geq \mathbb{P}(Y_{\tilde{x}} = y') / \mathbb{P}(Y_x = y')$ . In words, CS states that if  $y$  was observed and this outcome becomes relatively more likely than  $y'$  under the intervention, then the counterfactual outcome  $\tilde{Y}$  can not be  $y'$ .



Figure 2. A simple causal graph to illustrate CS.

Though somewhat appealing, the appropriateness of CS can depend on the application. First, CS is a very strong assumption that should be justified by domain specific knowledge. Second, and as we show in Example 1, CS can permit counterfactuals that it was seemingly designed to exclude.

**Example 1.** Consider Figure 2 and suppose  $X \in \{0, 1\}$  denotes a medical treatment and  $Y \in \{\text{bad}, \text{better}, \text{best}\}$  the patient outcome. For illustration, suppose the outcome  $Y_x$  obeys the following distribution:  $Y_0 \sim \{\text{bad}, \text{better}, \text{best}\}$  w.p.  $\{0.2, 0.3, 0.5\}$  and  $Y_1 \sim \{\text{bad}, \text{better}, \text{best}\}$  w.p.  $\{0.2, 0.2, 0.6\}$ . That is, under treatment, the “best” outcome becomes more likely but the likelihood of the “bad” outcome does not change. Consider a patient whose outcome  $Y$  was “better” under no treatment ( $x = 0$ ). Suppose also that domain specific knowledge tell us that even at the individual level, the counterfactual outcome  $\tilde{Y}$  should not be worse under treatment ( $\tilde{x} = 1$ ) than under no treatment ( $x = 0$ ). However, since

$$\frac{\mathbb{P}(Y_1 = \text{better})}{\mathbb{P}(Y_0 = \text{better})} = \frac{0.2}{0.3} < \frac{0.2}{0.2} = \frac{\mathbb{P}(Y_1 = \text{bad})}{\mathbb{P}(Y_0 = \text{bad})},$$

“bad” is a feasible counterfactual outcome under CS.

Even if CS is appropriate, its current operationalization has a key limitation. In particular, instead of considering all possible structural causal models (SCMs) that obey CS, both Oberst & Sontag (2019) and Tsirtsis et al. (2021) pick one SCM via the Gumbel-max distribution. Ideally, one should characterize the space of all SCMs obeying CS, and map that space into appropriate bounds on the CQI.

We present our optimization-based framework to perform counterfactual analysis next. Our framework does not rely on CS. However, if CS is deemed appropriate, our approach allows one to encode CS as linear constraints in the optimization and characterize the *entire* space of solutions that obey CS, which we do to negatively answer the open question of Oberst & Sontag (2019) regarding whether Gumbel-max obeys CS uniquely. Further, if enforcing the so-called *pathwise monotonicity* (PM) is desirable, i.e., ensuring the counterfactual outcome does not worsen under a better intervention (as we assumed in Example 1), then we can embed it in our optimization via linear constraints as well.

<sup>1</sup>Instead of using the “twin networks” approach (Pearl, 2009b), we perform the counterfactual analysis directly by leveraging the structure in our model.

## 4. Counterfactual Analysis via Optimization

We now present our solution methodology for the counterfactual analysis problem introduced in §2. We first discuss the underlying SCM (§4.1), which is a precursor to defining the counterfactual model  $\widetilde{\mathbf{M}}$  (§4.2), which feeds into our optimization framework for counterfactual analysis (§4.3).

### 4.1. The Structural Causal Model (SCM)

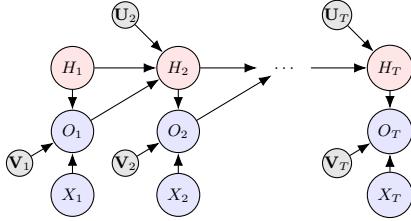


Figure 3. The SCM underlying the dynamic latent state model. The only difference between the SCM here and Figure 1 is the addition of (grey) exogenous noise nodes  $[\mathbf{U}_t, \mathbf{V}_t]_t$ .

To understand the SCM (Figure 3), consider  $O_t$  for any  $t$ , which is a stochastic function of its parents  $(H_t, X_t)$ . The stochasticity is driven by the exogenous noise vector  $\mathbf{V}_t := [V_{thx}]_{h,x}$ , which comprises of  $|\mathbb{H}||\mathbb{X}|$  noise variables. We model the exogenous node as a vector (as opposed to a scalar) to capture the fact that each  $O_{thx} := O_t | (H_t = h, X_t = x)$  defines a *distinct* random variable for all  $(h, x)$ . Moreover, these random variables might be independent, or they might display positive or negative dependence. One way to handle this is to associate each  $O_{thx}$  with a distinct noise variable  $V_{thx}$ . The *dependence structure* among these noise variables  $[V_{thx}]_{h,x}$  is then what determines the dependence structure among  $[O_{thx}]_{h,x}$ . The structural equation obeys

$$O_t = f(H_t, X_t, \mathbf{V}_t) = \sum_{h,x} f_{hx}(V_{thx}) \mathbb{I}_{\{H_t=h, X_t=x\}} \quad (3a)$$

where  $f_{hx}(\cdot)$  is defined using the emission distribution  $[e_{hxi}]_i$  and  $V_{thx} \sim \text{Unif}[0, 1]$  wlog. Similarly, for  $t > 1$ , recognizing that each  $H_{thi} := H_t | (H_{t-1} = h, O_{t-1} = i)$  is a distinct random variable for all  $(h, i)$ , we associate each  $H_{thi}$  with its own noise variable  $U_{thi}$ :

$$H_t = g(H_{t-1}, O_{t-1}, \mathbf{U}_t) = \sum_{h,i} g_{hi}(U_{thi}) \mathbb{I}_{\{H_{t-1}=h, O_{t-1}=i\}} \quad (3b)$$

where  $g_{hi}(\cdot)$  is defined using the transition distribution  $[q_{hih'}]_{h'}$  and  $U_{thi} \sim \text{Unif}[0, 1]$  wlog.

The representation in (3a) allows us to model  $[O_{thx}]_{h,x}$  and capture any dependence structure among these random variables by specifying the joint multivariate distribution of  $\mathbf{V}_t$ .

Since the univariate marginals of  $\mathbf{V}_t$  are known ( $\text{Unif}[0, 1]$ ), specifying the multivariate distribution amounts to specifying the dependence structure or *copula*. (Of course, the same comment applies to (3b) and  $\mathbf{U}_t$  as well.) For example, if the  $V_{thx}$ 's are mutually independent (the independence copula) and we have  $(H_t = h', X_t = x')$ , then inferring the conditional distribution of  $V_{th'x'}$  will tell us nothing about the  $V_{thx}$ 's for  $(h, x) \neq (h', x')$ . Alternatively, if  $V_{thx} = V_{th'x'}$  for all pairs  $(h, x)$  and  $(h', x')$ , then this models perfect positive dependency (the comonotonic copula) and inferring the conditional distribution of  $V_{th'x'}$  amounts to simultaneously inferring the conditional distribution of all the  $V_{thx}$ 's. We emphasize that we must work with the exogenous vectors  $(\mathbf{U}_t, \mathbf{V}_t)$  when doing a *counterfactual* analysis since different joint distributions of  $(\mathbf{U}_t, \mathbf{V}_t)$  will lead to (possibly very) different values of PN. If we are not doing a counterfactual analysis and only care about the joint distribution of a (subset of)  $(O_{1:T}, H_{1:T})$  then our analysis will only depend on the joint distribution of the  $(\mathbf{U}_t, \mathbf{V}_t)$ s via their known univariate marginals.

In our dynamic model, the emissions and the state transitions are time-independent. Thus, it is natural to also assume the copulas underlying  $\mathbf{V}_t$  and  $\mathbf{U}_t$  are time-independent. We refer to this property as *time consistency*. As such, we define the notation  $O_{hx} := O_t | (H_t = h, X_t = x)$  and  $H_{hi} := H_{t+1} | (H_t = h, O_t = i)$ .<sup>2</sup> Then,  $e_{hxi} = \mathbb{P}(O_{hx} = i)$  and  $q_{hih'} = \mathbb{P}(H_{hi} = h')$ .

While the copula view is useful from a conceptual point of view (since specifying copulas for  $\mathbf{U}_t$  and  $\mathbf{V}_t$  amounts to specifying an SCM), it is more convenient to work with an alternative construction of the SCM. This is because in discrete-state space models, there will be infinitely many joint distributions of  $\mathbf{V}$  (and  $\mathbf{U}$ ) that all lead to the same joint distribution of  $[O_{hx}]_{h,x}$  (and  $[H_{hi}]_{h,i}$ ). In other words, the joint distribution of  $[V_{hx}]_{h,x}$  does not uniquely identify the joint distribution of  $[O_{hx}]_{h,x}$ . This is a consequence of Sklar's Theorem from the theory of copulas and is discussed<sup>3</sup> further in §C. We will therefore take a more direct approach by modeling the unknown joint distribution of  $[O_{hx}]_{h,x}$  (and  $[H_{hi}]_{h,i}$ ). As such, we define

$$\theta_{\widetilde{h\bar{x}}, hx}(\widetilde{i}, i) := \mathbb{P}(O_{\widetilde{h\bar{x}}} = \widetilde{i}, O_{hx} = i) \quad (4a)$$

$$\pi_{\widetilde{h\bar{i}}, hi}(\widetilde{h}', h') := \mathbb{P}(H_{\widetilde{h\bar{i}}} = \widetilde{h}', H_{hi} = h'). \quad (4b)$$

We are now ready to discuss the counterfactual model. (Note that we only define the “pairwise marginals” in (4) as they will suffice for our purposes.)

<sup>2</sup> $O_t | (H_t = h, X_t = x)$  is time-independent and hence, we use the notation  $O_{hx}$  instead of  $O_{thx}$ . Same logic holds for  $H_{hi}$ .

<sup>3</sup>In §C, we also discuss specific copulas (e.g., independence and comonotonic copulas) that can be used to provide benchmark values of PN.

## 4.2. The Counterfactual Model $\widetilde{\mathbf{M}}$

Recall from §2 that  $\widetilde{\mathbf{M}}$  is obtained after the two steps of abduction (conditioning on the observed data  $(o_{1:T}, x_{1:T})$ ) and action (changing the policy from  $x_{1:T}$  to  $\widetilde{x}_{1:T}$ ). Understanding the dynamics underlying  $\widetilde{\mathbf{M}}$  are non-trivial, primarily due to the abduction step where the goal is to obtain the posterior distribution of the hidden path  $H_{1:T}$ . It is not possible to provide a closed-form expression for this distribution but we can use filtering / smoothing methods to describe the posterior dynamics of  $H_{1:T}$ . (See §B for details.)

We can therefore use these dynamics to generate  $B$  Monte-Carlo samples  $[h_{1:T}(b)]_{b=1}^B$  from the posterior, i.e., from the distribution of  $H_{1:T} \mid (o_{1:T}, x_{1:T})$ . Then, by conditioning on each sample  $b$ , it is possible to characterize  $\widetilde{\mathbf{M}}$ . In particular, denote by  $\widetilde{\mathbf{M}}(b) \equiv (\widetilde{\mathbf{p}}(b), [\widetilde{\mathbf{E}}^{(t)}(b)]_t, [\widetilde{\mathbf{Q}}^{(t)}(b)]_t)$  the counterfactual model corresponding to posterior sample  $h_{1:T}(b)$ . Similar to the primitives  $(\mathbf{p}, \mathbf{E}, \mathbf{Q})$  in §2, the counterfactual primitives  $(\widetilde{\mathbf{p}}(b), [\widetilde{\mathbf{E}}^{(t)}(b)]_t, [\widetilde{\mathbf{Q}}^{(t)}(b)]_t)$  correspond to initial state, emission, and transition distributions. As  $H_1$  in Figure 1 has no parents,  $\widetilde{\mathbf{p}}(b)$  is such that the counterfactual hidden state in period 1 equals the posterior sample  $h_1(b)$ , i.e.,  $\widetilde{h}_1(b) = h_1(b)$ . In contrast with  $\mathbf{E}$  and  $\mathbf{Q}$ , both  $\widetilde{\mathbf{E}}^{(t)}(b)$  and  $\widetilde{\mathbf{Q}}^{(t)}(b)$  are time-dependent (note the super-script “(t)”). This is because the period  $t$  counterfactual emission  $\widetilde{\mathbf{E}}^{(t)}(b) := [\widetilde{e}_{\widetilde{h}\widetilde{x}\widetilde{i}}^{(t)}(b)]_{\widetilde{h}, \widetilde{x}, \widetilde{i}}$  and transition  $\widetilde{\mathbf{Q}}^{(t)}(b) := [\widetilde{q}_{\widetilde{h}\widetilde{i}\widetilde{h}'}^{(t)}(b)]_{\widetilde{h}, \widetilde{i}, \widetilde{h}'}$  probabilities are as follows:

$$\widetilde{e}_{\widetilde{h}\widetilde{x}\widetilde{i}}^{(t)}(b) = \mathbb{P}(O_{\widetilde{h}\widetilde{x}} = \widetilde{i} \mid O_{h_t(b)x_t} = o_t) \quad (5a)$$

$$\widetilde{q}_{\widetilde{h}\widetilde{i}\widetilde{h}'}^{(t)}(b) = \mathbb{P}(H_{\widetilde{h}\widetilde{i}} = \widetilde{h}' \mid H_{h_t(b)o_t} = h_{t+1}(b)). \quad (5b)$$

(The  $O_{hx}$  and  $H_{hi}$  notation is defined above (4).) The dependence on  $t$  is through the observed data  $(o_t, x_t)$  and the posterior samples  $(h_t(b), h_{t+1}(b))$ . As such, for each posterior path  $b$ ,  $\widetilde{\mathbf{M}}(b)$  is a time-dependent dynamic latent state model. If we knew  $\widetilde{\mathbf{E}}^{(t)}(b)$  and  $\widetilde{\mathbf{Q}}^{(t)}(b)$ , then we could simulate  $\widetilde{\mathbf{M}}(b)$  to obtain a Monte-Carlo estimate of our CQI by averaging the CQI over the  $B$  posterior sample paths. However,  $\widetilde{\mathbf{E}}^{(t)}(b)$  and  $\widetilde{\mathbf{Q}}^{(t)}(b)$  are unknown as they depend on the joint distribution of  $(\mathbf{U}_t, \mathbf{V}_t)$ .

Towards this end, we can combine (5) with (4) to obtain

$$\begin{aligned} \widetilde{e}_{\widetilde{h}\widetilde{x}\widetilde{i}}^{(t)}(b) &= \frac{\theta_{\widetilde{h}\widetilde{x}, h_t(b)x_t}(\widetilde{i}, o_t)}{e_{h_t(b)x_t o_t}} \\ \widetilde{q}_{\widetilde{h}\widetilde{i}\widetilde{h}'}^{(t)}(b) &= \frac{\pi_{\widetilde{h}\widetilde{i}, h_t(b)o_t}(\widetilde{h}', h_{t+1}(b))}{q_{h_t(b)o_t h_{t+1}(b)}}, \end{aligned}$$

which expresses the unknown and time-dependent emission and transition distributions in terms of the unknown  $\theta$  and  $\pi$  that are time-independent.

## 4.3. Polynomial Optimization

We now propose an optimization model where we treat the unknowns  $(\theta, \pi)$  as decisions and maximize (minimize) the CQI to obtain an upperbound (lowerbound). We present our optimization model in terms of the objective and constraints, followed by a discussion on enforcing CS and PM.

**Objective.** As in (2), we wish to understand the PN, which equals  $\mathbb{P}(\widetilde{H}_T \neq 7)$ , where  $\widetilde{H}_T$  is the hidden state at time  $T$  under  $\widetilde{\mathbf{M}}$ . The randomness in  $\widetilde{H}_T$  depends on the randomness in (i) the true hidden path  $H_{1:T}$  (captured by  $[h_{1:T}(b)]_b$ ) and (ii) the counterfactual model  $\widetilde{\mathbf{M}} \mid H_{1:T}$  after conditioning on  $H_{1:T}$  (captured by  $\widetilde{\mathbf{M}}(b)$ ). Lemma 1 decomposes PN using these two uncertainties. (All proofs are in §A.)

**Lemma 1.** *We have*

$$PN = 1 - \lim_{B \rightarrow \infty} \frac{1}{B} \sum_{b=1}^B \mathbb{P}_{\widetilde{\mathbf{M}}(b)}(\widetilde{H}_T = 7).$$

We next express  $\mathbb{P}_{\widetilde{\mathbf{M}}(b)}(\widetilde{H}_T)$  in terms of  $(\theta, \pi)$  from (4).

**Lemma 2.** *For  $t \in \{T, T-1, \dots, 2\}$ ,  $\mathbb{P}_{\widetilde{\mathbf{M}}(b)}(\widetilde{h}_t) := \mathbb{P}_{\widetilde{\mathbf{M}}(b)}(\widetilde{H}_t = \widetilde{h}_t)$  obeys the following recursion (over  $t$ ):*

$$\begin{aligned} \mathbb{P}_{\widetilde{\mathbf{M}}(b)}(\widetilde{h}_t) &= \sum_{\widetilde{h}_{t-1}, \widetilde{o}_{t-1}} \frac{\pi_{\widetilde{h}_{t-1}\widetilde{o}_{t-1}, h_{t-1}(b)o_{t-1}}(\widetilde{h}_t, h_t(b))}{q_{h_{t-1}(b)o_{t-1} h_t(b)}} \times \\ &\quad \frac{\theta_{\widetilde{h}_{t-1}\widetilde{x}_{t-1}, h_{t-1}(b)x_{t-1}}(\widetilde{o}_{t-1}, o_{t-1})}{e_{h_{t-1}(b)x_{t-1} o_{t-1}}} \times \\ &\quad \mathbb{P}_{\widetilde{\mathbf{M}}(b)}(\widetilde{h}_{t-1}). \end{aligned}$$

*The recursion breaks at  $t = 1$ :*

$$\mathbb{P}_{\widetilde{\mathbf{M}}(b)}(\widetilde{h}_1) = \begin{cases} 1 & \text{if } \widetilde{h}_1 = h_1(b) \\ 0 & \text{otherwise.} \end{cases}$$

Putting together Lemmas 1 and 2 allows us to express PN in terms of the various primitives, all of which except  $(\theta, \pi)$  are known (or can be sampled). Thus, we use the notation  $\text{PN}(\theta, \pi \mid [h_{1:T}(b)]_b)$ . As soon as we fix  $(\theta, \pi)$ , we can estimate PN. However, it is unclear apriori what we should fix  $(\theta, \pi)$  at. We might have some information on the structure of  $(\theta, \pi)$  that can help us shrink their feasibility space but in general, there can be many  $(\theta, \pi)$ s that are “reasonable”. To overcome this lack of knowledge, we take an agnostic view and compute bounds over PN. The upper (lower) bound is computed by maximizing (minimizing)  $\text{PN}(\theta, \pi \mid [h_{1:T}(b)]_b)$  over the set of  $(\theta, \pi)$  that are “reasonable”. Denoting by  $\mathcal{F}$  the set of “reasonable”  $(\theta, \pi)$

(discussed next), we define

$$\text{PN}^{\text{ub}}(B) := \max_{(\boldsymbol{\theta}, \boldsymbol{\pi}) \in \mathcal{F}} \text{PN}(\boldsymbol{\theta}, \boldsymbol{\pi} \mid [h_{1:T}(b)]_b) \quad (6a)$$

$$\text{PN}^{\text{lb}}(B) := \min_{(\boldsymbol{\theta}, \boldsymbol{\pi}) \in \mathcal{F}} \text{PN}(\boldsymbol{\theta}, \boldsymbol{\pi} \mid [h_{1:T}(b)]_b). \quad (6b)$$

Both the optimizations in (6) are sample average approximations (SAA) due to the use of the Monte-Carlo samples  $[h_{1:T}(b)]_b$ . Thus,  $\text{PN}^{\text{ub}}(B)$  and  $\text{PN}^{\text{lb}}(B)$  are estimates of the “true”  $\text{PN}^{\text{ub}}$  and  $\text{PN}^{\text{lb}}$ . However, given  $[h_{1:T}(b)]_b$  are iid samples, the following consistency result is immediate (cf. Proposition 5.2 in Shapiro et al. (2021)).

**Proposition 1.**  $(\text{PN}^{\text{lb}}(B), \text{PN}^{\text{ub}}(B))$  converges to  $(\text{PN}^{\text{lb}}, \text{PN}^{\text{ub}})$  w.p. 1 as  $B \rightarrow \infty$ .

In addition, we can characterize the asymptotics of  $(\text{PN}^{\text{lb}}(B), \text{PN}^{\text{ub}}(B))$  via results in the SAA theory and we refer the reader to §5.1.2 of Shapiro et al. (2021).

**Constraints (feasibility set  $\mathcal{F}$ ).** We now shift our focus to the feasibility set  $\mathcal{F}$ . Since  $\boldsymbol{\theta}$  and  $\boldsymbol{\pi}$  consist of 2-dimensional joint PMFs, they must obey basic probability axioms. In particular, they must be non-negative and agree with their known 1-dimensional marginals so that

$$\sum_{h'} \pi_{\tilde{h}i, hi}(\tilde{h}', h') = q_{\tilde{h}i, h'} \forall (\tilde{h}, \tilde{i}, \tilde{h}') \forall (h, i) \quad (7a)$$

$$\sum_{\tilde{h}'} \pi_{\tilde{h}i, hi}(\tilde{h}', h') = q_{hi, h'} \forall (\tilde{h}, \tilde{i}) \forall (h, i, h') \quad (7b)$$

$$\sum_i \theta_{\tilde{h}\tilde{x}, hx}(\tilde{i}, i) = e_{\tilde{h}\tilde{x}} \forall (\tilde{h}, \tilde{x}, \tilde{i}) \forall (h, x) \quad (7c)$$

$$\sum_{\tilde{i}} \theta_{\tilde{h}\tilde{x}, hx}(\tilde{i}, i) = e_{hx} \forall (\tilde{h}, \tilde{x}) \forall (h, x, i). \quad (7d)$$

Recall that  $(\mathbf{Q}, \mathbf{E})$ , i.e., the right-hand-sides of (7), are known. Moreover, since  $\mathbf{Q}$  and  $\mathbf{E}$  themselves define 1-dimensional probability distributions and therefore sum to 1, (7) ensures the same will be true of all the 2-dimensional marginals in  $\boldsymbol{\theta}$  and  $\boldsymbol{\pi}$ , i.e., they will also sum to 1. In addition, we have

$$\pi_{hi, hi}(h', h') = q_{hi, h'} \forall (h, i, h') \quad (8a)$$

$$\theta_{hx, hx}(i, i) = e_{hx} \forall (h, x, i). \quad (8b)$$

To see why (8) holds, consider  $\pi_{hi, hi}(h', h')$  for example. By (4), this equals  $\mathbb{P}(H_{hi} = h', H_{hi} = h') = \mathbb{P}(H_{hi} = h') = q_{hi, h'}$ . Constraints in (8) can be interpreted as saying that counterfactual emissions and transitions must agree with the real-world emissions and transitions when the parent variables (as defined by the structure of the graphical model in Figure 3) coincide.

Let  $\mathcal{F}$  be the feasible region defined by the constraints (7) and (8) along with  $(\boldsymbol{\theta}, \boldsymbol{\pi}) \geq 0$ . Observe that  $\text{PN}(\boldsymbol{\theta}, \boldsymbol{\pi})$  is

a polynomial in  $(\boldsymbol{\theta}, \boldsymbol{\pi})$  and the constraints in (7) and (8) are linear. Thus, both the problems in (6) fall within the class of polynomial optimization (Anjos & Lasserre, 2011). Denoting by  $\text{PN}^*$  the PN under the true (unknown)  $(\boldsymbol{\theta}, \boldsymbol{\pi})$ , we obtain the following inequalities.

**Proposition 2.**  $\text{PN}^{\text{lb}} \leq \text{PN}^* \leq \text{PN}^{\text{ub}}$ .

**Enforcing CS and PM via linear constraints.** Suppose that at some time, the patient was in state  $h$ , the emission was  $i$ , followed by a transition to state  $h'$ . This maps to the realization  $H_{hi} = h'$ . For  $\tilde{h}' \neq h'$ , CS requires that if  $\mathbb{P}(H_{\tilde{h}i} = h') / \mathbb{P}(H_{hi} = h') \geq \mathbb{P}(H_{\tilde{h}i} = \tilde{h}') / \mathbb{P}(H_{hi} = \tilde{h}')$ , then  $\mathbb{P}(H_{\tilde{h}i} = \tilde{h}' \mid H_{hi} = h') = 0$ . Observe that the “if” condition is equivalent to  $q_{\tilde{h}i, h'} / q_{hi, h'} \geq q_{\tilde{h}i, \tilde{h}'} / q_{hi, \tilde{h}'}$  and the LHS of “then” equals  $\pi_{\tilde{h}i, hi}(\tilde{h}', h') / q_{hi, h'}$ . Hence, for the state transitions, CS is equivalent to adding the following linear constraints for all  $(h, i, h', \tilde{h}, \tilde{i}, \tilde{h}')$ :

$$\pi_{\tilde{h}i, hi}(\tilde{h}', h') = 0 \text{ if } \frac{q_{\tilde{h}i, h'}}{q_{hi, h'}} \geq \frac{q_{\tilde{h}i, \tilde{h}'}}{q_{hi, \tilde{h}'}}. \quad (9a)$$

Similarly, for emissions, CS can be modeled by adding the following linear constraints for all  $(h, x, i, \tilde{h}, \tilde{x}, \tilde{i})$ :

$$\theta_{\tilde{h}\tilde{x}, hx}(\tilde{i}, i) = 0 \text{ if } \frac{e_{\tilde{h}\tilde{x}}}{e_{hx}} \geq \frac{e_{\tilde{h}\tilde{x}}}{e_{hx}}. \quad (9b)$$

Hence, we characterize the space of all SCMs that obey CS, which is in contrast to picking just one such SCM (Oberst & Sontag, 2019). Enforcing CS naturally leads to tighter bounds, but the bounds may not be “legitimate” if the true  $(\boldsymbol{\theta}, \boldsymbol{\pi})$  does not satisfy CS. Denoting by  $\text{PN}_{\text{cs}}^{\text{ub}}$  and  $\text{PN}_{\text{cs}}^{\text{lb}}$  the bounds obtained by adding CS constraints (9) to the optimizations in (6), we have the following result.

**Proposition 3.**  $\text{PN}^{\text{lb}} \leq \text{PN}_{\text{cs}}^{\text{lb}} \leq \text{PN}_{\text{cs}}^{\text{ub}} \leq \text{PN}^{\text{ub}}$ .

PM can also be enforced via linear constraints. To see this, suppose the patient has in-situ cancer in period  $t$  which is not detected but the patient’s state remains at in-situ in period  $t + 1$ . Then, in the counterfactual world, if the cancer is detected in period  $t$ , then PM would require that the cancer can not be worse than in-situ in period  $t + 1$ , i.e.,

$$\mathbb{P}(H_{\tilde{h}i} = \tilde{h}' \mid H_{hi} = h') = 0$$

for  $h = 2, i \in \{1, 2\}, h' = 2, \tilde{h} \in \{2, 4\}, \tilde{i} = 4, \tilde{h}' \in \{5, 7\}$ . There can be multiple such cases to consider and we can enforce all the PM constraints by setting the corresponding  $\pi_{\tilde{h}i, hi}(\tilde{h}', h')$  variables equal to 0 as  $\pi_{\tilde{h}i, hi}(\tilde{h}', h') = \mathbb{P}(H_{hi} = h') \mathbb{P}(H_{\tilde{h}i} = \tilde{h}' \mid H_{hi} = h')$ . As with CS (Proposition 3), PM will result in bounds  $\text{PN}_{\text{pm}}^{\text{ub}}$  and  $\text{PN}_{\text{pm}}^{\text{lb}}$  tighter than  $\text{PN}^{\text{ub}}$  and  $\text{PN}^{\text{lb}}$ .

**Algorithm 1** Counterfactual analysis via optimization

**Require:**  $(\mathbf{E}, \mathbf{Q}), (o_{1:T}, x_{1:T}), B, \tilde{x}_{1:T}$   
 1:  $h_{1:T}(b) \sim H_{1:T} \mid (o_{1:T}, x_{1:T}) \forall b = 1, \dots, B$   
 2:  $\text{PN}^{\text{ub}}(B) = \max_{(\theta, \pi) \in \mathcal{F}} \text{PN}(\theta, \pi \mid [h_{1:T}(b)]_b)$   
 3:  $\text{PN}^{\text{lb}}(B) = \min_{(\theta, \pi) \in \mathcal{F}} \text{PN}(\theta, \pi \mid [h_{1:T}(b)]_b)$   
 4: **return**  $(\text{PN}^{\text{lb}}(B), \text{PN}^{\text{ub}}(B))$

We summarize our developments in Algorithm 1, which outputs the bounds  $(\text{PN}^{\text{lb}}(B), \text{PN}^{\text{ub}}(B))$ <sup>4</sup>. Line 1 (sampling) can be executed efficiently (cf. §B), and we discuss two computational considerations behind solving the polynomial optimizations (lines 2 and 3).

First, though the constraints are linear, the objective is polynomial, making it a non-trivial non-convex optimization problem. To solve it, we leverage state-of-the-art developments in optimization. In particular, we use the BARON solver (Sahinidis, 2023), which relies on a polyhedral branch-and-cut approach, allowing it to achieve global optima (Tawarmalani & Sahinidis, 2005). We found it to work well in our numerics (§5).

Second, in terms of the problem size, it follows immediately from (4) that we have *at most*  $|\mathbb{H}|^4|\mathbb{O}|^2 + |\mathbb{H}|^2|\mathbb{O}|^2|\mathbb{X}|^2$  variables ( $\pi$  and  $\theta$ ). Similarly, it follows from (7) and (8) that the feasible region  $\mathcal{F}$  is defined by *at most*  $2|\mathbb{H}|^3|\mathbb{O}|^2 + 2|\mathbb{H}|^2|\mathbb{O}||\mathbb{X}|^2 + |\mathbb{H}|^2|\mathbb{O}| + |\mathbb{H}||\mathbb{O}||\mathbb{X}|$  constraints. However, these are merely upper bounds and we can exploit the sparsity inherent in the underlying application to drastically reduce the problem size. For instance, in our breast cancer application, we have  $(|\mathbb{H}|, |\mathbb{O}|, |\mathbb{X}|) = (7, 7, 2)$ , with the above formulae giving 127,253 variables and 36,799 constraints. After we exploit sparsity (detailed in §5), both are reduced to under 2000. Further, as CS and PM can be modeled by setting appropriate variables to 0, they allow for further sparsity as we can delete those variables from the optimization.

## 5. Numerical Experiments

We now apply our approach to the breast cancer application we described in §1.

**Setup.** We described the elements of the underlying dynamic latent-state model  $\mathbf{M} \equiv (\mathbf{p}, \mathbf{E}, \mathbf{Q})$  in §2. It has a total of 7 states, 7 emissions, and 2 actions. Given patient-level data  $(o_{1:T}, x_{1:T})$ , we wish to estimate the PN as defined in (2). The primitives  $(\mathbf{p}, \mathbf{E}, \mathbf{Q})$  are calibrated to real-data using a mix of sources, which we discuss in §D.1.

<sup>4</sup>We can output  $(\text{PN}_{\text{cs}}^{\text{lb}}(B), \text{PN}_{\text{cs}}^{\text{ub}}(B))$  and  $(\text{PN}_{\text{pm}}^{\text{lb}}(B), \text{PN}_{\text{pm}}^{\text{ub}}(B))$  as well by solving the same optimization problems but with additional linear constraints.

We consider two paths with the first path defined as:

$$\underbrace{o_1}_{=2}, \underbrace{o_2, \dots, o_{T-2}, o_{T-1}}_{=1}, \underbrace{o_T}_{=7}$$

$$\underbrace{x_1}_{=0}, \underbrace{x_2, \dots, x_{T-2}, x_{T-1}}_{=1}, \underbrace{x_T}_{=0}$$

That is, we observe a negative test result in period 1 after which screening was not performed for  $T - 2$  periods (red font). The patient died from breast cancer in period  $T$ . Note that under this path, given the calibrated primitives in §D.1, it has to be the case that  $h_{T-1} = 3$  (undiagnosed invasive) since a transition from state 2 (undiagnosed in-situ) to 7 is impossible. Further, the transition from 3 to 7 is not unlikely ( $q_{317} \approx 0.15$ ). The second path is similar but with one difference: screening was performed in period  $T - 1$  and invasive cancer was detected:

$$\underbrace{o_1}_{=2}, \underbrace{o_2, \dots, o_{T-2}, o_{T-1}}_{=1}, \underbrace{o_T}_{=5}, \underbrace{o_T}_{=7}$$

$$\underbrace{x_1}_{=0}, \underbrace{x_2, \dots, x_{T-2}, x_{T-1}, x_T}_{=0}$$

Hence, in contrast with path 1, the final transition from invasive to death was under treatment with probability  $q_{357} \approx 0.01$  (§D.1), which is much smaller than  $q_{317}$  from above. Given that this low probability transition did occur, this suggests the patient had an “aggressive” cancer in path 2. As such, regardless of what the optimal  $\theta$  and  $\pi$  are, the chances of survival on the counterfactual path would be low because of this “aggressive” nature of the cancer. This doesn’t hold on path 1 as the cancer was less “aggressive”.

We vary  $T \in \{4, \dots, 10\}$ , with a larger value of  $T$  suggesting the cancer may have progressed more slowly and thus, resulting in a higher survival probability in the counterfactual world. We compute PN bounds using our framework (Algorithm 1), which we implemented in MATLAB (MATLAB, 2021). To solve the polynomial optimizations, we use the MATLAB-BARON interface (Sahinidis, 2023). It solved each of our problem instance to global optimality within 30 minutes, as indicated by its exitflags. We generated  $B = 500$  samples using our sampling method in §B. It took less than 2 seconds and we found  $B = 500$  was large enough to produce stable results. We ensured this stability by computing our results for 50 seeds (for each (path,  $T$ ) pair). We parallelized the computations over the 50 seeds on an HPC, which is equipped with Intel Xeon E5 processors. None of our jobs required more than 16 GB of RAM. As noted below Algorithm 1, the sparse structure of  $\mathbf{E}$  and  $\mathbf{Q}$  drastically reduces the size of the problem. For example, when considering the  $\pi_{\tilde{h}\tilde{i}, h\tilde{i}}(\tilde{h}', h')$  variables, we rule out the ones that map to impossible  $(h, i, h')$  or  $(\tilde{h}, \tilde{i}, \tilde{h}')$  combinations (refer to §D.1.2).

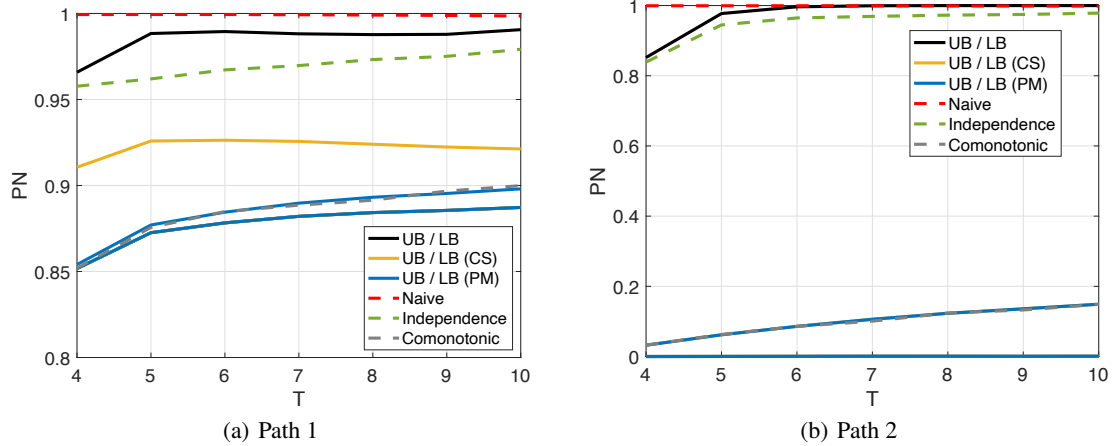


Figure 4. PN results for paths 1 and 2 as we vary  $T \in \{4, \dots, 10\}$ . In both the plots, the LB, LB (CS), and LB (PM) curves coincide (the lowest curves). In addition, for path 2, the UB (CS) and UB (PM) curves coincide as well. For each data point, we show the average over 50 seeds and note that the standard deviation (s.d.) for every data point is smaller than 0.02. Given this small magnitude, we omit the  $\pm 1$  s.d. bars to reduce the clutter in the sub-figures.

**Results.** The results are displayed in Figure 4, where we show the PN bounds for both paths as we vary  $T$ . In addition to the bounds  $(PN^{lb}, PN^{ub})$  computed via our baseline optimization (UB/LB), we show the bounds obtained when we encode CS (UB/LB (CS)) and PM (UB/LB (PM))<sup>5</sup>. We also show the PN estimate when we perform counterfactual simulations using the two copulas discussed in §C (independence and comonotonic)<sup>6</sup>. Finally, the naive estimate completely ignores the information in the observations, i.e., it does not execute the abduction step and is therefore an invalid estimate of PN.

We make two high-level observations in Figure 4. First, it is indeed the case that a higher  $T$  results in a higher PN, confirming our intuition from above. Second, the naive estimate is independent of the observed path (and can fall outside the bounds), which makes sense since it does not perform abduction but simply simulates the original model  $\mathbf{M}$  under the intervention policy  $\tilde{x}_{1:T} = 0$ .

For path 1, we get relatively tight bounds, with PN always above 0.85. This means that in the counterfactual world, the patient would have not died with high probability, consistent with our discussion around  $q_{317}$  above. Even in the absence of any additional structure such as CS or PM, the gap between the lower and upper bounds is within  $\sim 10$  percentage points. The gap gets tighter with CS (within  $\sim 5$  percentage points) and PM (within  $\sim 1$  percentage point!). The fact that the LB and UB under CS do not coincide resolves the open question of Oberst & Sontag (2019) regarding the unique-

<sup>5</sup>Details on the PM constraints for breast cancer are in §D.2.

<sup>6</sup>Further details on the comonotonic copula specific to the breast cancer model are in §D.3.

ness of Gumbel-max mechanism w.r.t. CS – it is not. It is not surprising that the comonotonic estimate falls within the PM bounds. Interestingly, the estimated PN for the two copulas (independence and comonotonic) roughly cover the range of possibilities in terms of the bounds.

For path 2, the lower bounds are close to 0. This aligns with the fact that despite being diagnosed in period  $T - 1$  (and hence, provided treatment), the patient eventually died (which suggests that the patient had an “aggressive” cancer). The bounds without CS and PM are relatively loose, simply reflecting the lack of knowledge to reason in a counterfactual world. As soon as we inject knowledge via CS or PM, the bounds become much tighter.

## 6. Concluding Remarks

We have provided a framework for performing counterfactual analysis in dynamic latent state models and in particular, computing lower and upper bounds on CQIs. There are several interesting directions for future research. First, can we use variance reduction methods and other Monte-Carlo techniques to improve our basic Monte Carlo approach for generating posterior sample paths? Second, can we leverage the structure of the optimization problem (a polynomial objective with linear constraints) to develop a solution procedure that is more efficient than using an off-the-shelf solver? Finally, on the practical front, it would be of interest to apply our framework to real-world medical applications and use domain-specific knowledge to obtain (via the imposition of additional constraints) tighter bounds on the CQIs.

## References

- Anjos, M. F. and Lasserre, J. B. *Handbook on semidefinite, conic and polynomial optimization*, volume 166. Springer Science & Business Media, 2011.
- Ayer, T., Alagoz, O., and Stout, N. K. A POMDP approach to personalize mammography screening decisions. *Operations Research*, 60(5):1019–1034, 2012.
- Balke, A. and Pearl, J. Counterfactual probabilities: Computational methods, bounds and applications. In *Uncertainty Proceedings*, pp. 46–54. San Francisco (CA), 1994.
- Barber, D. *Bayesian Reasoning and Machine Learning*. Cambridge University Press, 2012.
- Buesing, L., Weber, T., Zwols, Y., Heess, N., Racaniere, S., Guez, A., and Lespiau, J.-B. Woulda, coulda, shoulda: Counterfactually-guided policy search. In *International Conference on Learning Representations*, 2019.
- Cai, Z., Kuroki, M., Pearl, J., and Tian, J. Bounds on direct effects in the presence of confounded intermediate variables. *Biometrics*, 64(3):695–701, 2008.
- Haugh, M. B. and Lacedelli, O. R. Information relaxation bounds for partially observed Markov decision processes. *IEEE Transactions on Automatic Control*, 65(8):3256–3271, 2019.
- Johnstone, P. A., Norton, M. S., and Riffenburgh, R. H. Survival of patients with untreated breast cancer. *Journal of surgical oncology*, 73(4):273–277, 2000.
- Kaufman, S., Kaufman, J., MacLenose, R., Greenland, S., and Poole, C. Improved estimation of controlled direct effects in the presence of unmeasured confounding of intermediate variables. *Statistics in Medicine*, 25:1683–1702, 2005.
- Lorberbom, G., Johnson, D. D., Maddison, C. J., Tarlow, D., and Hazan, T. Learning generalized gumbel-max causal mechanisms. In Ranzato, M., Beygelzimer, A., Dauphin, Y., Liang, P., and Vaughan, J. W. (eds.), *Advances in Neural Information Processing Systems*, volume 34, pp. 26792–26803. Curran Associates, Inc., 2021.
- MATLAB. *Version 9.10.0 (R2021b)*. The MathWorks Inc., Natick, Massachusetts, 2021.
- McNeil, A. J., Frey, R., and Embrechts, P. *Quantitative Risk Management: Concepts, Techniques and Tools*. Princeton University Press, 2 edition, 2015.
- Mueller, S., Li, A., and Pearl, J. Causes of effects: Learning individual responses from population data. *arXiv*, 2021.
- Nelsen, R. *An Introduction to Copulas*. Springer, 2 edition, 2006.
- NIH. SEER Cancer Statistics Review (CSR) 1975-2017. 2020. URL [https://seer.cancer.gov/archive/csr/1975\\_2017/results\\_merged/sect\\_04\\_breast.pdf](https://seer.cancer.gov/archive/csr/1975_2017/results_merged/sect_04_breast.pdf).
- Oberst, M. and Sontag, D. Counterfactual off-policy evaluation with Gumbel-max structural causal models. In Chaudhuri, K. and Salakhutdinov, R. (eds.), *Proceedings of the 36th International Conference on Machine Learning*, volume 97 of *Proceedings of Machine Learning Research*, pp. 4881–4890. PMLR, 09–15 Jun 2019.
- Pearl, J. Causal inference in statistics: An overview. *Statistics surveys*, 3:96–146, 2009a.
- Pearl, J. *Causality*. Cambridge University Press, 2 edition, 2009b.
- Pearl, J. and Mackenzie, D. *The Book of Why*. Penguin Books, 2018.
- Sahinidis, N. V. *BARON 2023.1.5: Global Optimization of Mixed-Integer Nonlinear Programs*, User’s Manual, 2023.
- Shapiro, A., Dentcheva, D., and Ruszczyński, A. *Lectures on stochastic programming: modeling and theory*. SIAM, 2021.
- Sklar, A. Fonctions de répartition à n dimensions et leurs marges. *Publ. Inst. Statist. Univ. Paris*, 8:229–231, 1959.
- Sprague, B. L. and Trentham-Dietz, A. Prevalence of breast carcinoma in situ in the United States. *JAMA: the journal of the American Medical Association*, 302(8):846, 2009.
- Tawarmalani, M. and Sahinidis, N. V. A polyhedral branch-and-cut approach to global optimization. *Mathematical programming*, 103(2):225–249, 2005.
- Tian, J. and Pearl, J. Probabilities of causation: Bounds and identification. *Annals of Mathematics and Artificial Intelligence*, 8:287–313, 2000.
- Tsirtsis, S., De, A., and Rodriguez, M. Counterfactual explanations in sequential decision making under uncertainty. In Ranzato, M., Beygelzimer, A., Dauphin, Y., Liang, P., and Vaughan, J. W. (eds.), *Advances in Neural Information Processing Systems*, volume 34, pp. 30127–30139. Curran Associates, Inc., 2021.
- UWBCS. University of Wisconsin Breast Cancer Simulation Model. 2013. URL <https://resources.cisnet.cancer.gov/registry/packages/uwbc-wisconsin/>.
- Zhang, J., Tian, J., and Bareinboim, E. Partial counterfactual identification from observational and experimental data, 2021.

## A. Proofs

**Lemma 1.** *We have*

$$PN = 1 - \lim_{B \rightarrow \infty} \frac{1}{B} \sum_{b=1}^B \mathbb{P}_{\tilde{\mathbf{M}}(b)}(\tilde{H}_T = 7).$$

**Proof.** Observe that

$$\begin{aligned} PN &= \mathbb{P}_{\tilde{H}_T}(\tilde{H}_T \neq 7) && \text{[by definition]} \\ &= 1 - \mathbb{P}_{\tilde{H}_T}(\tilde{H}_T = 7) && [\mathbb{P}(Y \neq y) = 1 - \mathbb{P}(Y = y)] \\ &= 1 - \mathbb{E}_{\tilde{H}_T}[\mathbb{I}\{\tilde{H}_T = 7\}] && [\mathbb{P}(Y = y) = \mathbb{E}[\mathbb{I}\{Y = y\}]] \\ &= 1 - \mathbb{E}_{H_{1:T}}[\mathbb{E}_{\tilde{\mathbf{M}}|H_{1:T}}[\mathbb{I}\{\tilde{H}_T = 7\}]] && \text{[law of total expectation]} \\ &= 1 - \frac{1}{B} \sum_{b=1}^B \mathbb{P}_{\tilde{\mathbf{M}}(b)}(\tilde{H}_T = 7) \text{ as } B \rightarrow \infty. && \text{[law of large numbers]} \end{aligned}$$

The proof is now complete.  $\square$

**Lemma 2.** *For  $t \in \{T, T-1, \dots, 2\}$ ,  $\mathbb{P}_{\tilde{\mathbf{M}}(b)}(\tilde{h}_t) := \mathbb{P}_{\tilde{\mathbf{M}}(b)}(\tilde{H}_t = \tilde{h}_t)$  obeys the following recursion (over  $t$ ):*

$$\begin{aligned} \mathbb{P}_{\tilde{\mathbf{M}}(b)}(\tilde{h}_t) &= \sum_{\tilde{h}_{t-1}, \tilde{o}_{t-1}} \frac{\pi_{\tilde{h}_{t-1}, \tilde{o}_{t-1}, h_{t-1}(b), o_{t-1}}(\tilde{h}_t, h_t(b))}{q_{h_{t-1}(b), o_{t-1}, h_t(b)}} \times \\ &\quad \frac{\theta_{\tilde{h}_{t-1}, \tilde{x}_{t-1}, h_{t-1}(b), x_{t-1}}(\tilde{o}_{t-1}, o_{t-1})}{e_{h_{t-1}(b), x_{t-1}, o_{t-1}}} \times \\ &\quad \mathbb{P}_{\tilde{\mathbf{M}}(b)}(\tilde{h}_{t-1}). \end{aligned}$$

The recursion breaks at  $t = 1$ :

$$\mathbb{P}_{\tilde{\mathbf{M}}(b)}(\tilde{h}_1) = \begin{cases} 1 & \text{if } \tilde{h}_1 = h_1(b) \\ 0 & \text{otherwise.} \end{cases}$$

**Proof.** For  $t \in \{T, T-1, \dots, 2\}$ , observe that

$$\begin{aligned} \mathbb{P}_{\tilde{\mathbf{M}}(b)}(\tilde{h}_t) &= \sum_{\tilde{h}_{t-1} \in \mathbb{H}} \sum_{\tilde{o}_{t-1} \in \mathbb{O}} \mathbb{P}_{\tilde{\mathbf{M}}(b)}(\tilde{h}_t, \tilde{h}_{t-1}, \tilde{o}_{t-1}) \\ &= \sum_{\tilde{h}_{t-1} \in \mathbb{H}} \sum_{\tilde{o}_{t-1} \in \mathbb{O}} \mathbb{P}_{\tilde{\mathbf{M}}(b)}(\tilde{h}_t \mid \tilde{h}_{t-1}, \tilde{o}_{t-1}) \mathbb{P}_{\tilde{\mathbf{M}}(b)}(\tilde{o}_{t-1} \mid \tilde{h}_{t-1}) \mathbb{P}_{\tilde{\mathbf{M}}(b)}(\tilde{h}_{t-1}) \\ &= \sum_{\tilde{h}_{t-1} \in \mathbb{H}} \sum_{\tilde{o}_{t-1} \in \mathbb{O}} \tilde{q}_{\tilde{h}_{t-1}, \tilde{o}_{t-1}, \tilde{h}_t}^{(t-1)}(b) \times \tilde{e}_{\tilde{h}_{t-1}, \tilde{x}_{t-1}, \tilde{o}_{t-1}}^{(t-1)}(b) \times \mathbb{P}_{\tilde{\mathbf{M}}(b)}(\tilde{h}_{t-1}) \\ &= \sum_{\tilde{h}_{t-1} \in \mathbb{H}} \sum_{\tilde{o}_{t-1} \in \mathbb{O}} \frac{\pi_{\tilde{h}_{t-1}, \tilde{o}_{t-1}, h_{t-1}(b), o_{t-1}}(\tilde{h}_t, h_t(b))}{q_{h_{t-1}(b), o_{t-1}, h_t(b)}} \times \frac{\theta_{\tilde{h}_{t-1}, \tilde{x}_{t-1}, h_{t-1}(b), x_{t-1}}(\tilde{o}_{t-1}, o_{t-1})}{e_{h_{t-1}(b), x_{t-1}, o_{t-1}}} \times \mathbb{P}_{\tilde{\mathbf{M}}(b)}(\tilde{h}_{t-1}). \end{aligned}$$

The base case ( $t = 1$ ) holds since the counterfactual hidden state in period 1 equals the posterior sample  $h_1(b)$  (recall from §4.2). The proof is now complete.  $\square$

## B. Sampling Hidden Paths from the Posterior Distribution

In this section, we show how one can efficiently perform filtering, smoothing, and sampling for the dynamic latent state model in Figure 1. As our model is a generalization of an HMM (recall Remark 1), these algorithms are simple generalizations of the standard variants corresponding to an HMM (Barber, 2012).

**Filtering.** We first compute  $\alpha(h_t) := \mathbb{P}(h_t, o_{1:t}, x_{1:t})$  which will yield the un-normalized filtered posterior distribution. We can then easily normalize it to compute  $\mathbb{P}(h_t | o_{1:t}, x_{1:t}) \propto \alpha(h_t)$ . We begin with  $\alpha(h_1) := \mathbb{P}(o_1 | h_1, x_1)\mathbb{P}(h_1 | x_1)\mathbb{P}(x_1) = \mathbb{P}(o_1 | h_1, x_1)\mathbb{P}(h_1)\mathbb{P}(x_1)$ . For  $t > 1$ , note that

$$\begin{aligned} \alpha(h_t) &= \sum_{h_{t-1}} \mathbb{P}(h_t, h_{t-1}, o_{1:t-1}, o_t, x_{1:t}) \\ &= \sum_{h_{t-1}} \mathbb{P}(o_t | h_t, h_{t-1}, o_{1:t-1}, x_{1:t}) \mathbb{P}(h_t | h_{t-1}, o_{1:t-1}, x_{1:t}) \mathbb{P}(x_t | h_{t-1}, o_{1:t-1}, x_{1:t-1}) \mathbb{P}(h_{t-1}, o_{1:t-1}, x_{1:t-1}) \\ &= \sum_{h_{t-1}} \mathbb{P}(o_t | h_t, x_t) \mathbb{P}(h_t | h_{t-1}, o_{t-1}) \mathbb{P}(x_t) \mathbb{P}(h_{t-1}, o_{1:t-1}, x_{1:t-1}) \\ &= \mathbb{P}(x_t) \mathbb{P}(o_t | h_t, x_t) \sum_{h_{t-1}} \mathbb{P}(h_t | h_{t-1}, o_{t-1}) \alpha(h_{t-1}). \end{aligned}$$

**Smoothing.** We now compute  $\beta(h_t) := \mathbb{P}(o_{t+1:T}, x_{t+1:T} | h_t, o_t)$  with the understanding that  $\beta(h_T) = 1$ . For  $t < T$ , we have

$$\begin{aligned} \beta(h_t) &= \sum_{h_{t+1}} \mathbb{P}(o_{t+1}, x_{t+1}, o_{t+2:T}, x_{t+2:T}, h_{t+1} | h_t, o_t) \\ &= \sum_{h_{t+1}} \mathbb{P}(o_{t+2:T}, x_{t+2:T} | h_t, o_t, h_{t+1}, o_{t+1}, x_{t+1}) \mathbb{P}(h_{t+1}, o_{t+1}, x_{t+1} | h_t, o_t) \\ &= \sum_{h_{t+1}} \mathbb{P}(o_{t+2:T}, x_{t+2:T} | h_{t+1}, o_{t+1}) \mathbb{P}(o_{t+1} | h_{t+1}, x_{t+1}, h_t, o_t) \mathbb{P}(h_{t+1}, x_{t+1} | h_t, o_t) \\ &= \sum_{h_{t+1}} \beta(h_{t+1}) \mathbb{P}(o_{t+1} | h_{t+1}, x_{t+1}) \mathbb{P}(x_{t+1} | h_{t+1}, h_t, o_t) \mathbb{P}(h_{t+1} | h_t, o_t) \\ &= \mathbb{P}(x_{t+1}) \sum_{h_{t+1}} \beta(h_{t+1}) \mathbb{P}(o_{t+1} | h_{t+1}, x_{t+1}) \mathbb{P}(h_{t+1} | h_t, o_t). \end{aligned}$$

Now, note that

$$\begin{aligned} \mathbb{P}(h_t, o_{1:T}, x_{1:T}) &= \mathbb{P}(h_t, o_{1:t}, x_{1:t}) \mathbb{P}(o_{t+1:T}, x_{t+1:T} | h_t, o_{1:t}, x_{1:t}) \\ &= \mathbb{P}(h_t, o_{1:t}, x_{1:t}) \mathbb{P}(o_{t+1:T}, x_{t+1:T} | h_t, o_t) \\ &= \alpha(h_t) \beta(h_t). \end{aligned}$$

We therefore obtain the hidden state marginal

$$\mathbb{P}(h_t | o_{1:T}, x_{1:T}) = \frac{\alpha(h_t) \beta(h_t)}{\sum_{h_t} \alpha(h_t) \beta(h_t)},$$

which solves the smoothing problem.

**Pairwise marginal.** We can compute  $\mathbb{P}(h_t, h_{t+1} | o_{1:T}, x_{1:T})$  by noting that

$$\begin{aligned} \mathbb{P}(h_t, h_{t+1} | o_{1:T}, x_{1:T}) &\propto \mathbb{P}(o_{1:t}, o_{t+1}, o_{t+2:T}, x_{1:t}, x_{t+1}, x_{t+2:T}, h_{t+1}, h_t) \\ &= \mathbb{P}(o_{t+2:T}, x_{t+2:T} | o_{1:t}, o_{t+1}, x_{1:t}, x_{t+1}, h_{t+1}, h_t) \mathbb{P}(o_{1:t}, o_{t+1}, x_{1:t}, x_{t+1}, h_{t+1}, h_t) \\ &= \mathbb{P}(o_{t+2:T}, x_{t+2:T} | h_{t+1}, o_{t+1}) \mathbb{P}(o_{t+1} | o_{1:t}, h_{t+1}, h_t, x_{1:t}, x_{t+1}) \mathbb{P}(o_{1:t}, h_{t+1}, h_t, x_{1:t}, x_{t+1}) \\ &= \mathbb{P}(o_{t+2:T}, x_{t+2:T} | h_{t+1}, o_{t+1}) \mathbb{P}(o_{t+1} | h_{t+1}, x_{t+1}) \mathbb{P}(h_{t+1}, x_{t+1} | o_{1:t}, x_{1:t}, h_t) \mathbb{P}(o_{1:t}, x_{1:t}, h_t) \\ &= \mathbb{P}(o_{t+2:T}, x_{t+2:T} | h_{t+1}, o_{t+1}) \mathbb{P}(o_{t+1} | h_{t+1}, x_{t+1}) \mathbb{P}(h_{t+1}, x_{t+1} | h_t, o_t) \mathbb{P}(o_{1:t}, x_{1:t}, h_t). \end{aligned} \tag{12}$$

We can rearrange (12) to obtain

$$\mathbb{P}(h_t, h_{t+1} | o_{1:T}, x_{1:T}) \propto \alpha(h_t) \mathbb{P}(o_{t+1} | h_{t+1}, x_{t+1}) \mathbb{P}(h_{t+1}, x_{t+1} | h_t, o_t) \beta(h_{t+1}). \tag{13}$$

Therefore,  $\mathbb{P}(h_t, h_{t+1} | o_{1:T}, x_{1:T})$  is easy to compute once the forward-backward, i.e. the filtering and smoothing, recursions have been completed.

**Sampling.** We would like to sample from the posterior  $\mathbb{P}(h_{1:T} \mid o_{1:T}, x_{1:T})$ . We can do this by first noting that

$$\begin{aligned} \mathbb{P}(h_{1:T} \mid o_{1:T}, x_{1:T}) &= \mathbb{P}(h_1 \mid h_{2:T}, o_{1:T}, x_{1:T}) \dots \mathbb{P}(h_{T-1} \mid h_T, o_{1:T}, x_{1:T}) \mathbb{P}(h_T \mid o_{1:T}, x_{1:T}) \\ &= \mathbb{P}(h_1 \mid h_2, o_{1:T}, x_{1:T}) \dots \mathbb{P}(h_{T-1} \mid h_T, o_{1:T}, x_{1:T}) \mathbb{P}(h_T \mid o_{1:T}, x_{1:T}). \end{aligned}$$

We can therefore sample sequentially via the following two steps:

- First, draw  $h_T$  from  $\mathbb{P}(h_T \mid o_{1:T}, x_{1:T})$ , which we know from the smoothed distribution of  $h_T$ .
- Second, observe that for any  $t < T$ , we have

$$\begin{aligned} \mathbb{P}(h_t \mid h_{t+1}, o_{1:T}, x_{1:T}) &\propto \mathbb{P}(h_t, h_{t+1} \mid o_{1:T}, x_{1:T}) \\ &\propto \alpha(h_t) \mathbb{P}(h_{t+1}, x_{t+1} \mid h_t, o_t) && \text{[by (13)]} \\ &= \alpha(h_t) \mathbb{P}(h_{t+1} \mid h_t, o_t) \mathbb{P}(x_{t+1}), \end{aligned}$$

from which it is easy to sample.

Hence, we can efficiently generate samples  $[h_{1:T}(b)]_{b=1}^B$  from the posterior  $\mathbb{P}(h_{1:T} \mid o_{1:T}, x_{1:T})$ .

## C. A Brief Introduction to Copulas

Copulas are functions that enable us to separate the marginal distributions from the dependency structure of a given multivariate distribution. They are particularly useful in applications where the marginal distributions are known (either from domain specific knowledge or because there is sufficient marginal data) but a joint distribution with these known marginals is required. In our application in this paper, we know the marginal distribution of each random variable in  $[O_{hx}]_{h,x}$  and  $[H_{hi}]_{h,i}$ , which is dictated by the model primitives  $(\mathbf{E}, \mathbf{Q})$  as follows:  $e_{hxi} = \mathbb{P}(O_{hx} = i)$  and  $q_{hih'} = \mathbb{P}(H_{hi} = h')$ . Indeed, these marginal distributions can be estimated from data, but the *joint distribution* must be specified in order to compute counterfactuals.

In each of these cases, one needs to work with a joint distribution with fixed or pre-specified marginal distributions. Copulas and Sklar's Theorem (see below) can be very helpful in these situations. We only briefly review some of the main results from the theory of copulas here but Nelsen (2006) can be consulted for an introduction to the topic. McNeil et al. (2015) also contains a nice introduction but in the context of financial risk management.

**Definition 1.** A  $d$ -dimensional copula,  $C : [0, 1]^d \rightarrow [0, 1]$  is a cumulative distribution function with uniform marginals.

We write  $C(\mathbf{u}) = C(u_1, \dots, u_d)$  for a generic copula. It follows immediately from Definition 1 that  $C(u_1, \dots, u_d)$  is non-decreasing in each argument and that  $C(1, \dots, 1, u_i, 1, \dots, 1) = u_i$ . It is also easy to confirm that  $C(1, u_1, \dots, u_{d-1})$  is a  $(d-1)$ -dimensional copula and, more generally, that all  $k$ -dimensional marginals with  $2 \leq k \leq d$  are copulas. The most important result from the theory of copulas is Sklar's Theorem (Sklar, 1959).

**Theorem 1 (Sklar 1959).** Consider a  $d$ -dimensional CDF  $\mathbf{\Pi}$  with marginals  $\mathbf{\Pi}_1, \dots, \mathbf{\Pi}_d$ . Then, there exists a copula  $C$  such that

$$\mathbf{\Pi}(x_1, \dots, x_d) = C(\mathbf{\Pi}_1(x_1), \dots, \mathbf{\Pi}_d(x_d)) \quad (14)$$

for all  $x_i \in [-\infty, \infty]$  and  $i = 1, \dots, d$ .

If  $\mathbf{\Pi}_i$  is continuous for all  $i = 1, \dots, d$ , then  $C$  is unique; otherwise  $C$  is uniquely determined only on  $\text{Ran}(\mathbf{\Pi}_1) \times \dots \times \text{Ran}(\mathbf{\Pi}_d)$ , where  $\text{Ran}(\mathbf{\Pi}_i)$  denotes the range of the CDF  $\mathbf{\Pi}_i$ .

Conversely, consider a copula  $C$  and univariate CDF's  $\mathbf{\Pi}_1, \dots, \mathbf{\Pi}_d$ . Then,  $\mathbf{\Pi}$  as defined in (14) is a multivariate CDF with marginals  $\mathbf{\Pi}_1, \dots, \mathbf{\Pi}_d$ .

A particularly important aspect of Sklar's Theorem in the context of this paper is that  $C$  is only uniquely determined on  $\text{Ran}(\mathbf{\Pi}_1) \times \dots \times \text{Ran}(\mathbf{\Pi}_d)$ . Because we are interested in applications with discrete state-spaces, this implies that there will be many copulas that lead to the same joint distribution  $\mathbf{\Pi}$ . It is for this reason that we prefer to work directly with the joint distribution of  $[O_{hx}]_{h,x}$  and  $[H_{hi}]_{h,i}$  (recall (4)). That said, we emphasize that specifying copulas for the exogenous vectors  $\mathbf{U}_t$  and  $\mathbf{V}_t$  is equivalent to specifying a particular structural causal model (SCM) in which any CQI can be computed.

The following important result was derived independently by Fréchet and Hoeffding and provides lower and upper bounds on copulas.

**Theorem 2 (The Fréchet-Hoeffding Bounds).** *Consider a copula  $C(\mathbf{u}) = C(u_1, \dots, u_d)$ . Then,*

$$\max \left\{ 1 - d + \sum_{i=1}^d u_i, 0 \right\} \leq C(\mathbf{u}) \leq \min\{u_1, \dots, u_d\}.$$

Three important copulas are the comonotonic, countermonotonic (only when  $d = 2$ ) and independence copulas which model extreme positive dependency, extreme negative dependency and (not surprisingly) independence. They are defined as follows.

**Comonotonic Copula.** The comonotonic copula is given by

$$C^P(\mathbf{u}) := \min\{u_1, \dots, u_d\}, \quad (15)$$

which coincides with the Fréchet-Hoeffding upper bound. It corresponds to the case of extreme positive dependence. For example, let  $\mathbf{U} = (U_1, \dots, U_d)$  with  $U_1 = U_2 = \dots = U_d \sim \text{Unif}[0, 1]$ . Then, clearly  $\min\{u_1, \dots, u_d\} = \mathbf{\Pi}(u_1, \dots, u_d)$  but by Sklar's Theorem  $F(u_1, \dots, u_d) = C(u_1, \dots, u_d)$  and so,  $C(u_1, \dots, u_d) = \min\{u_1, \dots, u_d\}$ .

**Countermonotonic Copula.** The countermonotonic copula is a 2-dimensional copula given by

$$C^N(\mathbf{u}) := \max\{u_1 + u_2 - 1, 0\}, \quad (16)$$

which coincides with the Fréchet-Hoeffding lower bound when  $d = 2$ . It corresponds to the case of extreme negative dependence. It is easy to check that (16) is the joint distribution of  $(U, 1 - U)$  where  $U \sim \text{Unif}[0, 1]$ . (The Fréchet-Hoeffding lower bound is only tight when  $d = 2$ . This is analogous to the fact that while a pairwise correlation can lie anywhere in  $[-1, 1]$ , the *average* pairwise correlation of  $d$  random variables is bounded below by  $-1/(d - 1)$ .)

**Independence Copula.** The independence copula satisfies

$$C^I(\mathbf{u}) := \prod_{i=1}^d u_i,$$

and it is easy to confirm using Sklar's Theorem that random variables are independent if and only if their copula is the independence copula.

A well known and important result regarding copulas is that they are invariant under monotonic transformations.

**Proposition 4 (Invariance Under Monotonic Transformations).** *Suppose the random variables  $X_1, \dots, X_d$  have continuous marginals and copula  $C_X$ . Let  $T_i : \mathbb{R} \rightarrow \mathbb{R}$ , for  $i = 1, \dots, d$  be strictly increasing functions. Then, the dependence structure of the random variables*

$$Y_1 := T_1(X_1), \dots, Y_d := T_d(X_d)$$

*is also given by the copula  $C_X$ .*

This leads immediately to the following result.

**Proposition 5.** *Let  $X_1, \dots, X_d$  be random variables with continuous marginals and suppose  $X_i = T_i(X_1)$  for  $i = 2, \dots, d$  where  $T_2, \dots, T_d$  are strictly increasing transformations. Then,  $X_1, \dots, X_d$  have the comonotonic copula.*

**Proof.** Apply the *invariance under monotonic transformations* proposition and observe that the copula of  $(X_1, X_1, \dots, X_1)$  is the comonotonic copula.  $\square$

Our framework in §4 implicitly optimizes over the space of copulas by solving polynomial programs with possibly a large number of variables and constraints. (We saw in §4.3 that the number of variables and constraints is polynomial in  $|\mathbb{H}|, |\mathbb{O}|$ )

and  $|\mathbb{X}|$  when calculating the probability of necessity (PN).) It may also be worthwhile, however, working explicitly with copulas. For example, the independence and comonotonic copulas are well understood and using these copulas to define SCMs may provide interesting benchmarks. Indeed, we estimate the PN for these benchmarks in our numerical results of §5. Towards this end, in §C.1 and §C.2, we explain how we can simulate our dynamic latent state model to estimate the CQI under the independence (§C.1) and comonotonic (§C.2) copulas. Specifically, we assume each of the copulas for  $\mathbf{U}_t$  and  $\mathbf{V}_t$  are the independence copulas in §C.1, whereas in §C.2, we assume their copulas are the comonotonic copula.

There is no reason, however, why we couldn't combine them and assume, for example, that the copula for  $\mathbf{U}_t$  was the independence copula and the copula for  $\mathbf{V}_t$  was the comonotonic copula. More generally, we could use domain-specific knowledge to identify or narrow down sub-components of the copulas and leave the remaining components to be identified via the optimization problems. Since convex combinations of copulas are copulas, we could also optimize over such combinations. For example, suppose domain specific knowledge<sup>7</sup> tells us that the copula of  $\mathbf{V}_t$  is  $\lambda C^N + (1 - \lambda)C^I$ , i.e., a convex combination of the comonotonic and independence copulas, with  $\lambda \in [0, 1]$  unknown. Then, the optimization over  $\mathbf{V}_t$  would reduce to a single-variable ( $\lambda$ ) optimization with a linear constraint. Of course, the optimization over the copula of  $\mathbf{U}_t$  must also be included but domain-specific knowledge may also help to simplify and constrain that component of the optimization. Properties such as pathwise monotonicity (PM) and counterfactual stability (CS) can also be expressed in copula terms. Indeed, PM can be expressed via the comonotonic copula, as we discuss in §C.2.

### C.1. Counterfactual Simulations Under the Independence Copula

For convenience, we copy Figure 3 from the main text, which is now labelled as Figure 5. Furthermore, recall that  $(o_{1:T}, x_{1:T})$  is the observed data and  $\tilde{x}_{1:T}$  is the intervention policy that was applied.

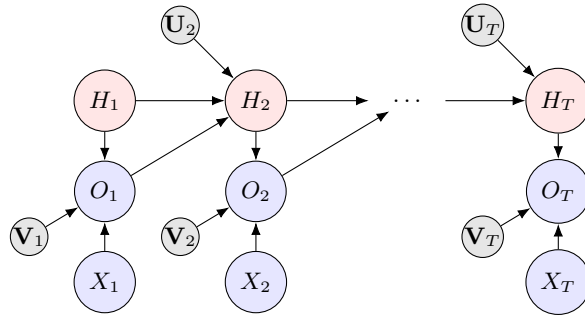


Figure 5. The SCM underlying the dynamic latent state model.

As in §4, we start with the posterior samples  $[h_{1:T}(b)]_{b=1}^B$  corresponding to the random path  $H_{1:T} \mid (o_{1:T}, x_{1:T})$ . These samples can be generated efficiently (cf. §B). For each sample  $b$ , our goal is to convert the sampled path  $h_{1:T}(b)$  into a counterfactual path  $\tilde{h}_{1:T}(b)$ . As noted in §4.2, irrespective of the copula choice, the counterfactual hidden state in period 1 equals the posterior sample, i.e.,

$$\tilde{h}_1(b) = h_1(b).$$

We next need to sample  $\tilde{h}_2(b)$ , but that first requires us to sample the counterfactual emission  $\tilde{o}_1(b)$  (cf. Figure 5). With the copula underlying  $\mathbf{V}_1$  being the independence copula, it follows that

$$\tilde{o}_1(b) = \begin{cases} o_1 & \text{if } x_1 = \tilde{x}_1 \text{ and } h_1(b) = \tilde{h}_1(b) \\ \text{sample from the emission distribution } [e_{\tilde{h}_1(b)\tilde{x}_1}^i]_i & \text{otherwise.} \end{cases}$$

The counterfactual emission  $\tilde{o}_1(b)$  allows us to sample the counterfactual state  $\tilde{h}_2(b)$ , which again leverages the fact that the copula underlying  $\mathbf{U}_2$  is the independence copula:

$$\tilde{h}_2(b) = \begin{cases} h_2(b) & \text{if } h_1(b) = \tilde{h}_1(b) \text{ and } o_1 = \tilde{o}_1(b) \\ \text{sample from the transition distribution } [q_{\tilde{h}_1(b)\tilde{o}_1(b)h'}]_{h'} & \text{otherwise.} \end{cases}$$

<sup>7</sup>It may be more likely that we only have domain specific knowledge over sub-components of the copulas (which are themselves copulas).

We then generate period 2 counterfactual emission  $\tilde{o}_2(b)$  in a similar manner and the process repeats until we hit the end of horizon. We summarize the procedure in Algorithm 2.

---

**Algorithm 2** Counterfactual simulations under the independence copula
 

---

**Require:**  $(\mathbf{E}, \mathbf{Q}), (o_{1:T}, x_{1:T}), [h_{1:T}(b)]_{b=1}^B, \tilde{x}_{1:T}$

- 1: **for**  $b = 1$  to  $B$  **do**
- 2:    $\tilde{h}_1(b) = h_1(b)$
- 3:   **for**  $t = 1$  to  $T - 1$  **do**
- 4:     **if**  $x_t = \tilde{x}_t$  and  $h_t(b) = \tilde{h}_t(b)$  **then**
- 5:        $\tilde{o}_t(b) = o_t$
- 6:     **else**
- 7:        $\tilde{o}_t(b) \sim \text{Categorical}([e_{\tilde{h}_t(b)\tilde{x}_t i}]_i)$
- 8:     **end if**
- 9:     **if**  $h_t(b) = \tilde{h}_t(b)$  and  $o_t = \tilde{o}_t(b)$  **then**
- 10:       $\tilde{h}_{t+1}(b) = h_{t+1}(b)$
- 11:     **else**
- 12:       $\tilde{h}_{t+1}(b) \sim \text{Categorical}([q_{\tilde{h}_t(b)\tilde{o}_t(b)h'}]_{h'})$
- 13:     **end if**
- 14:   **end for**
- 15: **end for**
- 16: **return**  $[\tilde{h}_{1:T}(b)]_b$

---

## C.2. Counterfactual Simulations Under the Comonotonic Copula

Before the formal description (which involves non-trivial notation), we provide the intuition (which is relatively straightforward). We do so by revisiting Example 1, where we have the causal graph  $X \rightarrow Y$  with  $X \in \{0, 1\}$  (medical treatment) and  $Y \in \{\text{bad}, \text{better}, \text{best}\}$  (patient outcome). The outcome  $Y_x := Y \mid (X = x)$  obeys the following distribution:  $Y_0 \sim \{\text{bad}, \text{better}, \text{best}\}$  w.p.  $\{0.2, 0.3, 0.5\}$  and  $Y_1 \sim \{\text{bad}, \text{better}, \text{best}\}$  w.p.  $\{0.2, 0.2, 0.6\}$ . The underlying SCM is shown again in Figure 6.

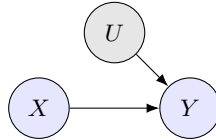


Figure 6. SCM for Example 1 with the comonotonic copula and hence, the noise node is a scalar  $U \sim \text{Unif}[0, 1]$ , as opposed to a vector  $\mathbf{U}$ . The structural equation is  $Y = f(X, U)$ , which we denote by  $f_X(U)$ , the *inverse transform* function corresponding to the random variable  $Y_X$ . That is,  $f_0(u) = \text{bad}, \text{better}, \text{and best}$  if  $u \in [0, 0.2], u \in [0.2, 0.5], \text{and } u \in [0.5, 1]$ , respectively. Similarly,  $f_1(u) = \text{bad}, \text{better}, \text{and best}$  if  $u \in [0, 0.2], u \in [0.2, 0.4], \text{and } u \in [0.4, 1]$ , respectively.

Consider a patient whose outcome  $Y$  was “better” under no treatment ( $x = 0$ ). Given the prior  $U \sim \text{Unif}[0, 1]$ , we get the posterior  $U \mid (Y_0 = \text{better}) \sim \text{Unif}[0.2, 0.5]$ . Now, suppose we are interested in the understanding the counterfactual outcome under the intervention  $\tilde{x} = 1$ , i.e., the random variable  $\tilde{Y} := Y_1 \mid (Y_0 = \text{better})$ . Then, given the  $\text{Unif}[0.2, 0.5]$  belief over  $U$  and the functional form of  $f_1(\cdot)$  (as defined in the caption of Figure 6), we get that the  $[0.2, 0.4]$  region of  $U$  will map to “better” and the  $[0.4, 0.5]$  to “best”. Hence,  $\tilde{Y}$  equals “better” w.p.  $2/3$  and “best” w.p.  $1/3$ . This clearly obeys the pathwise monotonicity (PM) intuition we alluded to towards the end of Example 1 (“the counterfactual outcome  $\tilde{Y}$  should not be worse under treatment ( $\tilde{x} = 1$ ) than under no treatment ( $x = 0$ )”).

We now formalize this intuition to our dynamic latent state model. As a prerequisite to discussing the notion of PM, one needs to define an ordering of the states (set  $\mathbb{H}$ ) and the emissions (set  $\mathbb{O}$ ), e.g., from “best” to “worst”. Denote by  $r_H(h)$  the rank of state  $h$  with respect to this ordering and by  $r_O(i)$  the rank of emission  $i$ . Furthermore, let  $r_H^{-1}(r)$  and  $r_O^{-1}(r)$  denote the inverse functions corresponding to  $r_H(h)$  and  $r_O(i)$ , respectively. That is,  $r_H^{-1}(r)$  returns the state with rank  $r$  and  $r_O^{-1}(r)$  returns the emission with rank  $r$ . Also, for each  $(h, i)$  pair, observe that  $[q_{hih'}]_{h'}$  denotes the transition distribution

(which maps to the random variable  $H_{hi}$ ). Corresponding to this distribution, define the rank-ordered CDF as follows:

$$Q_{hjh'} := \sum_{h'' : r_H(h'') \leq r_H(h')} q_{hjh''} \quad \forall h'. \quad (17a)$$

Similarly, for each  $(h, x)$  pair, observe that  $[e_{hxi}]_i$  denotes the emission distribution (which maps to the random variable  $O_{hx}$ ). Corresponding to this distribution, define the rank-ordered CDF as follows:

$$E_{hxi} := \sum_{j : r_O(j) \leq r_O(i)} e_{hxj} \quad \forall i. \quad (17b)$$

Also, define  $Q_{hi0} = E_{hx0} = 0$  for all  $(h, i)$  and  $(h, x)$ . We discuss these orderings for the breast cancer application in §D.3.

As in §C.1, we start with the posterior samples  $[h_{1:T}(b)]_{b=1}^B$  corresponding to the random path  $H_{1:T} \mid (o_{1:T}, x_{1:T})$ . For each sample  $b$ , our goal is to convert the sampled path  $h_{1:T}(b)$  into a counterfactual path  $\tilde{h}_{1:T}(b)$ . As noted in §4.2, irrespective of the copula choice, the counterfactual hidden state in period 1 equals the posterior sample, i.e.,

$$\tilde{h}_1(b) = h_1(b).$$

To generate  $\tilde{o}_1(b)$ , we revisit the SCM in Figure 7, which now has the noise nodes as scalars (as opposed to vectors). This is a direct implication of the comonotonic copula - see the statement immediately below (15).

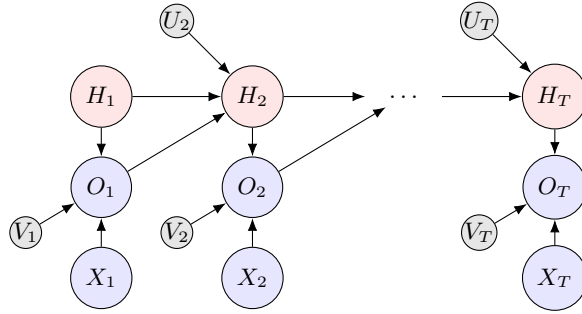


Figure 7. The SCM with the comonotonic copula. The key change is that the noise nodes are now scalars as opposed to vectors, i.e.,  $(U_t, V_t)$  as opposed to  $(\mathbf{U}_t, \mathbf{V}_t)$ .

By the structural equation (3a),  $\tilde{o}_1(b)$  equals

$$\tilde{o}_1(b) = f(\tilde{h}_1(b), \tilde{x}_1, V_1) = f_{\tilde{h}_1(b)\tilde{x}_1}(V_1), \quad (18a)$$

where  $f_{hx}(\cdot)$  is the inverse transform function corresponding to the rank-ordered CDF  $[E_{hxi}]_i$  (recall (17b)). Hence, all we need to sample  $\tilde{o}_1(b)$  is the posterior distribution of  $V_1$ , where the “posterior” corresponds to conditioning on  $O_{1h_1(b)x_1} = o_1$  (recall the notation  $O_{thx}$  from §4). Given the prior  $V_1 \sim \text{Unif}[0, 1]$ , we can compute the posterior in closed-form. In particular,

$$V_1 \mid (O_{1h_1(b)x_1} = o_1) \sim \text{Unif}[E_{h_1(b)x_1 o_1^-}, E_{h_1(b)x_1 o_1}], \quad (18b)$$

where  $o^- := r_O^{-1}(r_O(o) - 1)$  is the emission ranked just below  $o$ . Hence, we can efficiently sample  $V_1$  from its posterior, and this  $V_1$  sample can be used to generate  $\tilde{o}_1(b)$  (via (18a)). Given we encoded rank orderings in the CDF  $E_{hxi}$ , such sampling will naturally enforce pathwise monotonicity.

We can sample  $\tilde{h}_2(b)$  similarly. By the structural equation (3b),  $\tilde{h}_2(b)$  equals

$$\tilde{h}_2(b) = g(\tilde{h}_1(b), \tilde{o}_1, U_2) = g_{\tilde{h}_1(b)\tilde{o}_1}(U_2), \quad (19a)$$

where  $g_{hi}(\cdot)$  is the inverse transform function corresponding to the rank-ordered CDF  $[Q_{hjh'}]_{h'}$  (recall (17a)). Hence, all we need to sample  $\tilde{h}_2(b)$  is the posterior distribution of  $U_2$ , where the “posterior” corresponds to conditioning on

$H_{2h_1(b)o_1} = h_2(b)$  (recall the notation  $H_{thi}$  from §4). Given the prior  $U_2 \sim \text{Unif}[0, 1]$ , we can compute the posterior in closed-form. In particular,

$$U_2 \mid (H_{2h_1(b)o_1} = h_2(b)) \sim \text{Unif}[Q_{h_1(b)o_1h_2(b)^-}, Q_{h_1(b)o_1h_2(b)}], \quad (19b)$$

where  $h^- := r_H^{-1}(r_H(h) - 1)$  is the state ranked just below  $h$ . Hence, we can efficiently sample  $U_2$  from its posterior, and this  $U_2$  sample can be used to generate  $\tilde{h}_2(b)$  (via (19a)). Given we encoded rank orderings in the CDF  $Q_{h_ih'}$ , such sampling will naturally enforce pathwise monotonicity.

We then generate period 2 counterfactual emission  $\tilde{o}_2(b)$  in a similar manner and the process repeats until we hit the end of horizon. We summarize the procedure in Algorithm 3.

---

**Algorithm 3** Counterfactual simulations under the comonotonic copula

---

**Require:**  $(\mathbf{E}, \mathbf{Q})$ ,  $(o_{1:T}, x_{1:T})$ ,  $[h_{1:T}(b)]_{b=1}^B$ ,  $\tilde{x}_{1:T}$ ,  $r_H(\cdot)$ ,  $r_O(\cdot)$

```

1: for  $b = 1$  to  $B$  do
2:    $\tilde{h}_1(b) = h_1(b)$ 
3:   for  $t = 1$  to  $T - 1$  do
4:      $v_t \sim \text{Unif}[E_{\tilde{h}_t(b)x_t o_t^-}, E_{\tilde{h}_t(b)x_t o_t}]$  % posterior sample of  $V_t$  (see (18b))
5:      $\tilde{o}_t(b) = f_{\tilde{h}_t(b)\tilde{x}_t}(v_t)$  % counterfactual emission (see (18a))
6:      $u_{t+1} \sim \text{Unif}[Q_{\tilde{h}_t(b)o_t h_{t+1}(b)^-}, Q_{\tilde{h}_t(b)o_t h_{t+1}(b)}]$  % posterior sample of  $U_t$  (see (19b))
7:      $\tilde{h}_{t+1}(b) = g_{\tilde{h}_t(b)\tilde{o}_t}(u_{t+1})$  % counterfactual state (see (19a))
8:   end for
9: end for
10: return  $[\tilde{h}_{1:T}(b)]_b$ 

```

---

## D. Further Details on the Breast Cancer Case Study

### D.1. Model Primitives and Their Calibration

As discussed in §2, the breast cancer application has  $|\mathbb{H}| = 7$  states,  $|\mathbb{O}| = 7$  emissions, and  $|\mathbb{X}| = 2$  actions. To be consistent with the literature (Ayer et al., 2012), we treat each period as corresponding to 6 months. The model comprises of three primitives:  $\mathbf{p}$ ,  $\mathbf{Q}$ , and  $\mathbf{E}$ . We discuss their (sparse) structure and the calibration to real-data in §D.1.1, §D.1.2, and §D.1.3, respectively.

#### D.1.1. INITIAL STATE DISTRIBUTION $\mathbf{p}$

We have  $\mathbf{p} := (p_1, \dots, p_7)$  where  $p_h := \mathbb{P}(H_1 = h)$  for all  $h$ . Usually, breast cancer screening starts around the age of 40 and the prevalence among females aged 40-49 is 1.0183% (Table 4.24 of NIH (2020), all races, females):

$$p_2 + p_3 = 0.010183.$$

Since in-situ cancer comprises 20% of new breast cancer diagnoses (Sprague & Trentham-Dietz, 2009), we get

$$p_2 = 0.2 \times 0.010183$$

$$p_3 = 0.8 \times 0.010183.$$

It is natural to set

$$p_4 = p_5 = p_6 = p_7 = 0$$

and hence,

$$p_1 = 1 - p_2 - p_3 = 1 - 0.010183.$$

#### D.1.2. TRANSITION DISTRIBUTION $\mathbf{Q}$

We have  $\mathbf{Q} := [q_{h_ih'}]_{h,i,h'}$  with  $q_{h_ih'} := \mathbb{P}(H_{t+1} = h' \mid H_t = h, O_t = i)$ . Before discussing the calibration, we discuss the sparse structure of  $\mathbf{Q}$ . To do so, we define the transition matrix  $\mathbf{Q}(i) := [q_{h_ih'}]_{hh'}$  for each emission  $i$  (so that each row sums to 1) and observe that we have the following structure:



For  $q_{12}$ , we use the in-situ incidence rates from Table 4.12 of NIH (2020) (all races, females). For  $q_{13}$ , we use the invasive incidence rates from Table 4.11 of NIH (2020) (all races, females). The reported numbers are per year and we should divide by 2 to convert to a 6-month scale:

$$q_{12} = \frac{1}{2} \times \frac{33.0}{100000}$$

$$q_{13} = \frac{1}{2} \times \frac{128.5}{100000}.$$

Note that consistent with the 20-80 split in  $(p_2, p_3)$ , we have  $q_{13} \approx 4q_{12}$ .

**State 2 (undiagnosed in-situ cancer).** We are interested in  $(q_{22}, q_{23}, q_{27})$  (if cancer is not detected) and  $(q_{24}, q_{25}, q_{26}, \bar{q}_{27})$  (if cancer is detected). First, consider  $(q_{22}, q_{23}, q_{27})$ . Table 4.13 of NIH (2020) and Page 26 of UWBCS (2013) imply there is no death from in-situ cancer:

$$q_{27} = 0.$$

Haugh & Lacedelli (2019) assumed  $q_{23}$  to equal the invasive incidence rate  $q_{13}$  and so do we:

$$q_{23} = q_{13}$$

$$q_{22} = 1 - q_{23} - q_{27} = 1 - q_{13}.$$

Second, consider  $(q_{24}, q_{25}, q_{26}, \bar{q}_{27})$ . As  $q_{27} = 0$  and we expect  $\bar{q}_{27} \leq q_{27}$  (recall comment #4 above), we set

$$\bar{q}_{27} = 0.$$

As all in-situ cancer patients survive (if treated), no one transitions to invasive (if in-situ detected):

$$q_{25} = 0.$$

Finally, we have

$$q_{24} + q_{26} = 1.$$

The split between  $q_{24}$  and  $q_{26}$  is irrelevant in terms of the patient dying or not (all will survive as there is no positive probability path from state 4 to death; this will become clear when we discuss state 4 below).

**State 3 (undiagnosed invasive cancer).** We are interested in  $(q_{33}, q_{37})$  (if cancer is not detected) and  $(q_{35}, q_{36}, \bar{q}_{37})$  (if cancer is detected). First, consider  $(q_{33}, q_{37})$ .  $q_{37}$  is the probability of dying from invasive breast cancer (under no treatment). According to Johnstone et al. (2000), the 5-year and 10-year survival rates for invasive breast cancer patients (under no treatment) are 18.4% and 3.6%, respectively. On calibrating to 5-year rate, we get  $(1 - q_{37})^{10} = 0.184$ , which implies  $q_{37} \approx 15.6\%$  (note that we use “10” in the exponent since our time periods correspond to 6 months and hence, 5 years correspond to 10 periods). Similarly, on calibrating to 10-year rate, we get  $(1 - q_{37})^{20} = 0.036$  implies  $q_{37} \approx 15.3\%$ . The two calibrations are consistent with each other (lending evidence to time-invariance). Minimizing sum of squared errors over the two data points, i.e.,  $\min_{q_{37} \in [0,1]} \{((1 - q_{37})^{10} - 0.184)^2 + ((1 - q_{37})^{20} - 0.036)^2\}$ , gives the following estimate:

$$q_{37} = 0.1554.$$

Naturally, we have

$$q_{33} = 1 - q_{37}.$$

Second, consider  $(q_{35}, q_{36}, \bar{q}_{37})$ .  $q_{36}$  and  $\bar{q}_{37}$  are the probabilities of recovering and dying from invasive breast cancer (under treatment). Table 4.14 of NIH (2020) has various survival rates we can use to calibrate. We calibrate using the 10 data points corresponding to the year 2007 (see Figure 8):

$$q_{36} = 0.0459$$

$$\bar{q}_{37} = 0.0113.$$

As a sanity check, note that  $\bar{q}_{37} < q_{37}$ . Finally,

$$q_{35} = 1 - q_{36} - \bar{q}_{37}.$$



Having discussed the structure of  $\mathbf{E}$ , we now calibrate it to real-data. There are 3 parameters:  $e_{12}$ ,  $e_{24}$ , and  $e_{35}$ . All of them can be age specific but we ignore that.  $e_{12}$  is the *specificity* of the mammogram screening (i.e., probability of a true negative) and we calibrate it using Table 3 of Ayer et al. (2012):

$$e_{12} = 0.9.$$

$e_{24}$  is the in-situ *sensitivity* (i.e., probability of a true positive) and we calibrate it using Table 3 of Ayer et al. (2012):

$$e_{24} = 0.8.$$

Finally,  $e_{35}$  is the invasive sensitivity and following Ayer et al. (2012), we set

$$e_{35} = e_{24}.$$

## D.2. Details on the Pathwise Monotonicity (PM) Constraints

PM can be enforced via linear constraints. We briefly discussed this in §4.3 and now discuss all underlying PM constraints we embedded in our breast cancer numerics.

Recalling our §4.3 discussion for convenience, suppose the patient has in-situ cancer in period  $t$  which is not detected but the patient's state remains at in-situ in period  $t + 1$ . Then, in the counterfactual world, if the cancer is detected in period  $t$ , then PM would require that the cancer can not be worse than in-situ in period  $t + 1$ , i.e.,

$$\mathbb{P}(H_{\tilde{h}i} = \tilde{h}' \mid H_{hi} = h') = 0$$

for  $h = 2$ ,  $i \in \{1, 2\}$ ,  $h' = 2$ ,  $\tilde{h} \in \{2, 4\}$ ,  $\tilde{i} = 4$ ,  $\tilde{h}' \in \{5, 7\}$ . There can be multiple such cases to consider and we can enforce all the PM constraints by setting the corresponding  $\pi_{\tilde{h}i, h'}(\tilde{h}', h')$  variables equal to 0 as  $\pi_{\tilde{h}i, h'}(\tilde{h}', h') = \mathbb{P}(H_{hi} = h')\mathbb{P}(H_{\tilde{h}i} = \tilde{h}' \mid H_{hi} = h')$ .

Hence, to provide details on which all PM constraints we enforce, it suffices to enumerate the  $(h, i, h', \tilde{h}, \tilde{i}, \tilde{h}')$  combinations for which we set the  $\pi_{\tilde{h}i, h'}(\tilde{h}', h')$  variables equal to 0. To do so, we iterate over each state  $h \in \{1, \dots, 7\}$ . (Note that for PM, there are no  $(h, x, i, \tilde{h}, \tilde{x}, \tilde{i})$  combinations for which we set the  $\theta_{\tilde{h}x, hx}(\tilde{i}, i)$  variables equal to 0.)

**State  $h = 1$  (healthy).** We enforce PM for the following combinations:

- If  $(h, i, h')$  equals (healthy, whatever emission, healthy), then the counterfactual state  $\tilde{h}'$  can not be in-situ, invasive, or death if  $\tilde{h}$  is healthy. That is,  $h = 1$ ,  $i \in \mathbb{O}$ ,  $h' = 1$ ,  $\tilde{h} = 1$ ,  $\tilde{i} \in \mathbb{O}$ , and  $\tilde{h}' \in \{2, 3, 4, 5, 7\}$ .
- If  $(h, i, h')$  equals (healthy, whatever emission, in-situ), then the counterfactual state  $\tilde{h}'$  can not be healthy, invasive, or death if  $\tilde{h}$  is healthy. That is,  $h = 1$ ,  $i \in \mathbb{O}$ ,  $h' = 2$ ,  $\tilde{h} = 1$ ,  $\tilde{i} \in \mathbb{O}$ , and  $\tilde{h}' \in \{1, 3, 5, 7\}$ .
- If  $(h, i, h')$  equals (healthy, whatever emission, invasive), then the counterfactual state  $\tilde{h}'$  can not be healthy, in-situ, or death if  $\tilde{h}$  is healthy. That is,  $h = 1$ ,  $i \in \mathbb{O}$ ,  $h' = 3$ ,  $\tilde{h} = 1$ ,  $\tilde{i} \in \mathbb{O}$ , and  $\tilde{h}' \in \{1, 2, 4, 7\}$ .
- If  $(h, i, h')$  equals (healthy, whatever emission, death), then the counterfactual state  $\tilde{h}'$  can not be healthy, in-situ, or invasive if  $\tilde{h}$  is healthy. That is,  $h = 1$ ,  $i \in \mathbb{O}$ ,  $h' = 7$ ,  $\tilde{h} = 1$ ,  $\tilde{i} \in \mathbb{O}$ , and  $\tilde{h}' \in \{1, 2, 3, 4, 5\}$ .

**State  $h = 2$  (undiagnosed in-situ).** We enforce PM for the following combinations:

- If  $(h, i, h')$  equals (in-situ, undetected, in-situ), then the counterfactual state  $\tilde{h}'$  can not be invasive or death if  $\tilde{h}$  is healthy or in-situ. That is,  $h = 2$ ,  $i \in \{1, 2, 3\}$ ,  $h' = 2$ ,  $\tilde{h} \in \{1, 2, 4\}$ ,  $\tilde{i} \in \mathbb{O}$ , and  $\tilde{h}' \in \{3, 5, 7\}$ .
- If  $(h, i, h')$  equals (in-situ, detected, in-situ), then the counterfactual state  $\tilde{h}'$  can not be invasive or death if  $\tilde{h}$  is in-situ and detected. That is,  $h = 2$ ,  $i = 4$ ,  $h' = 4$ ,  $\tilde{h} \in \{2, 4\}$ ,  $\tilde{i} = 4$ , and  $\tilde{h}' \in \{3, 5, 7\}$ .

- If  $(h, i, h')$  equals (in-situ, undetected, invasive), then the counterfactual state  $\tilde{h}'$  can not be death if  $\tilde{h}$  is healthy or in-situ. That is,  $h = 2, i \in \{1, 2, 3\}, h' = 3, \tilde{h} \in \{1, 2, 4\}, \tilde{i} \in \mathbb{O}$ , and  $\tilde{h}' = 7$ .
- If  $(h, i, h')$  equals (in-situ, detected, invasive), then the counterfactual state  $\tilde{h}'$  can not be death if  $\tilde{h}$  is in-situ and detected. That is,  $h = 2, i = 4, h' = 5, \tilde{h} \in \{2, 4\}, \tilde{i} = 4$ , and  $\tilde{h}' = 7$ .
- If  $(h, i, h')$  equals (in-situ, detected, recovered), then the counterfactual state  $\tilde{h}'$  can not be in-situ, invasive, or death if  $\tilde{h}$  is in-situ and detected. That is,  $h = 2, i = 4, h' = 6, \tilde{h} \in \{2, 4\}, \tilde{i} = 4$ , and  $\tilde{h}' \in \{2, 3, 4, 5, 7\}$ .
- If  $(h, i, h')$  equals (in-situ, undetected, death), then the counterfactual state  $\tilde{h}'$  can not be in-situ, invasive, or recovered if  $\tilde{h}$  is in-situ and undetected. That is,  $h = 2, i \in \{1, 2, 3\}, h' = 7, \tilde{h} = 2, \tilde{i} \in \{1, 2, 3\}$ , and  $\tilde{h}' \in \{2, 3, 4, 5, 6\}$ .
- If  $(h, i, h')$  equals (in-situ, detected, death), then the counterfactual state  $\tilde{h}'$  can not be in-situ, invasive, or recovered if  $\tilde{h}$  is in-situ and detected. That is,  $h = 2, i = 4, h' = 7, \tilde{h} \in \{2, 4\}, \tilde{i} = 4$ , and  $\tilde{h}' \in \{2, 3, 4, 5, 6\}$ .

**State  $h = 3$  (undiagnosed invasive).** We enforce PM for the following combinations:

- If  $(h, i, h')$  equals (invasive, undetected, invasive), then the counterfactual state  $\tilde{h}'$  can not be death if  $\tilde{h}$  is healthy, in-situ, or invasive. That is,  $h = 3, i \in \{1, 2, 3\}, h' = 3, \tilde{h} \in \{1, 2, 3, 4, 5\}, \tilde{i} \in \mathbb{O}$ , and  $\tilde{h}' = 7$ .
- If  $(h, i, h')$  equals (invasive, detected, invasive), then the counterfactual state  $\tilde{h}'$  can not be death if  $\tilde{h}$  is invasive and detected. That is,  $h = 3, i = 5, h' = 5, \tilde{h} \in \{3, 5\}, \tilde{i} = 5$ , and  $\tilde{h}' = 7$ .
- If  $(h, i, h')$  equals (invasive, detected, recovered), then the counterfactual state  $\tilde{h}'$  can not be invasive or death if  $\tilde{h}$  is invasive and detected. That is,  $h = 3, i = 5, h' = 6, \tilde{h} \in \{3, 5\}, \tilde{i} = 5$ , and  $\tilde{h}' \in \{3, 5, 7\}$ .
- If  $(h, i, h')$  equals (invasive, undetected, death), then the counterfactual state  $\tilde{h}'$  can not be invasive or recovered if  $\tilde{h}$  is invasive and undetected. That is,  $h = 3, i \in \{1, 2, 3\}, h' = 7, \tilde{h} \in \{3, 5\}, \tilde{i} \in \{1, 2, 3\}$ , and  $\tilde{h}' \in \{3, 5, 6\}$ .
- If  $(h, i, h')$  equals (invasive, detected, death), then the counterfactual state  $\tilde{h}'$  can not be invasive or recovered if  $\tilde{h}$  is invasive and detected. That is,  $h = 3, i = 5, h' = 7, \tilde{h} \in \{3, 5\}, \tilde{i} = 5$ , and  $\tilde{h}' \in \{3, 5, 6\}$ .

**State  $h = 4$  (diagnosed in-situ).** We enforce PM for the following combinations:

- If  $(h, i, h')$  equals (in-situ, detected, in-situ), then the counterfactual state  $\tilde{h}'$  can not be invasive, recovered, or death if  $\tilde{h}$  is in-situ and detected. That is,  $h = 4, i = 4, h' = 4, \tilde{h} \in \{2, 4\}, \tilde{i} = 4$ , and  $\tilde{h}' \in \{5, 6, 7\}$ .
- If  $(h, i, h')$  equals (in-situ, detected, invasive), then the counterfactual state  $\tilde{h}'$  can not be in-situ, recovered, or death if  $\tilde{h}$  is in-situ and detected. That is,  $h = 4, i = 4, h' = 5, \tilde{h} \in \{2, 4\}, \tilde{i} = 4$ , and  $\tilde{h}' \in \{4, 6, 7\}$ .
- If  $(h, i, h')$  equals (in-situ, detected, recovery), then the counterfactual state  $\tilde{h}'$  can not be in-situ, invasive, or death if  $\tilde{h}$  is in-situ and detected. That is,  $h = 4, i = 4, h' = 6, \tilde{h} \in \{2, 4\}, \tilde{i} = 4$ , and  $\tilde{h}' \in \{4, 5, 7\}$ .
- If  $(h, i, h')$  equals (in-situ, detected, death), then the counterfactual state  $\tilde{h}'$  can not be in-situ, invasive, or recovered if  $\tilde{h}$  is in-situ and detected. That is,  $h = 4, i = 4, h' = 7, \tilde{h} \in \{2, 4\}, \tilde{i} = 4$ , and  $\tilde{h}' \in \{4, 5, 6\}$ .

**State  $h = 5$  (diagnosed invasive).** We enforce PM for the following combinations:

- If  $(h, i, h')$  equals (invasive, detected, invasive), then the counterfactual state  $\tilde{h}'$  can not be recovered or death if  $\tilde{h}$  is invasive and detected. That is,  $h = 5, i = 5, h' = 5, \tilde{h} \in \{3, 5\}, \tilde{i} = 5$ , and  $\tilde{h}' \in \{6, 7\}$ .
- If  $(h, i, h')$  equals (invasive, detected, recovery), then the counterfactual state  $\tilde{h}'$  can not be invasive or death if  $\tilde{h}$  is invasive and detected. That is,  $h = 5, i = 5, h' = 6, \tilde{h} \in \{3, 5\}, \tilde{i} = 5$ , and  $\tilde{h}' \in \{5, 7\}$ .
- If  $(h, i, h')$  equals (invasive, detected, death), then the counterfactual state  $\tilde{h}'$  can not be invasive or recovery if  $\tilde{h}$  is invasive and detected. That is,  $h = 5, i = 5, h' = 7, \tilde{h} \in \{3, 5\}, \tilde{i} = 5$ , and  $\tilde{h}' \in \{5, 6\}$ .

**State  $h = 6$  (recovery).** No combination for which we enforce PM.

**State  $h = 7$  (death).** No combination for which we enforce PM.

### D.3. Details on the Comonotonic Copula

We discussed the counterfactual simulation under the comonotonic copula for a general dynamic latent state model in §C.2. In this section, we connect that discussion to the breast cancer application. To do so, it suffices to define the rank functions  $r_H(\cdot)$  (for states) and  $r_O(\cdot)$  (for emissions). For states, there are two possible orderings that seem “natural” (from “best” to “worst”):

- (1, 6, 4, **2**, 5, 3, 7)
- (1, 6, 4, **5**, 2, 3, 7).

Recalling the  $\mathbf{Q}(i)$  notation from §D.1, observe that columns 2 and 5 are never “active” simultaneously in any row of  $\mathbf{Q}(i)$  (for any  $i$ ). Hence, the choice of ordering (between the two orderings above) will not matter and we can pick any one. Suppose we pick the first one. Then, this ordering defines the rank function. For example,  $r_H(6) = 2$ , i.e., rank of state 6 equals 2. For the inverse function,  $r_H^{-1}(2) = 6$ .

It is unclear how to define  $r_O(\cdot)$  for the breast cancer application but as it turns out, it does not matter. To see why, consider the generic path of interest (from (1)):

$$\underbrace{o_1, \dots, o_{\tau_s-1}}_{\in \{2,3\}}, \underbrace{o_{\tau_s}, \dots, o_{\tau_e}}_{=1}, \underbrace{o_{\tau_e+1}, \dots, o_{\tau_d-1}}_{\in \{4,5\}}, \underbrace{o_{\tau_d:T}}_{=7}.$$

For the first  $\tau_s - 1$  periods, observe that the counterfactual emission  $\tilde{o}_{1:\tau_s-1}(b)$  equals the observed emission  $o_{1:\tau_s-1}$  for each  $b$ . This is because the intervention policy  $\tilde{x}_{1:\tau_s-1}$  equals the observed policy  $x_{1:\tau_s-1}$ . Now, consider periods  $\tau_s$  to  $\tau_e$ , during which the screening was not done, i.e.,  $x_{\tau_s:\tau_e} = 1$ . Hence, the emissions  $o_{\tau_s:\tau_e} = 1$  w.p. 1 (see the matrix  $\mathbf{E}(1)$  in §D.1.3). This means that the emissions does not contain any information regarding the underlying noise variables  $V_{\tau_s:\tau_e}$  (see Figure 7) and hence, their posterior equals their prior, which is  $\text{Unif}[0, 1]$ . As such, for  $t \in \{\tau_s, \dots, \tau_e\}$ , we can sample  $\tilde{o}_t(b)$  using the categorical distribution over the probability vector  $[e_{\tilde{h}_t(b)\tilde{x}_t i}]_i$ . Note that we can use  $\tilde{o}_{\tau_s-1}(b)$  to sample  $\tilde{h}_{\tau_s}(b)$ , which we can use to sample  $\tilde{o}_{\tau_s}(b)$ , and so on (until we have sampled  $\tilde{h}_{\tau_e+1}(b)$ ). Now, consider  $t = \tau_e + 1$ . We know  $o_t \in \{4, 5\}$ :

- If  $o_t = 4$ , then  $h_t(b) = 2$  and  $\tilde{h}_t(b) \in \{2, 4, 6\}$  (cf. pathwise monotonicity).
  - If  $\tilde{h}_t(b) \in \{4, 6\}$ , then  $\tilde{o}_t(b) = \tilde{h}_t(b)$  (since rows 4 and 6 of  $\mathbf{E}(0)$  have 1 on the diagonal).
  - Else, if  $\tilde{h}_t(b) = 2 (= h_t(b))$ , then  $\tilde{o}_t(b) = o_t = 4$ .
- Else, if  $o_t = 5$ , then  $h_t(b) = 3$  and  $\tilde{h}_t(b) \in \{3, 4, 5, 6\}$  (cf. pathwise monotonicity).
  - If  $\tilde{h}_t(b) \in \{4, 5, 6\}$ , then  $\tilde{o}_t(b) = \tilde{h}_t(b)$  (since rows 4, 5, 6 of  $\mathbf{E}(0)$  have 1 on the diagonal).
  - If  $\tilde{h}_t(b) = 3 (= h_t(b))$ , then  $\tilde{o}_t(b) = o_t = 5$ .

Finally, for  $t \geq \tau_e + 2$ , we know  $h_t(b) \geq 4$  and that the corresponding rows in  $\mathbf{E}(0)$  are 0-1. Hence, the posterior of  $V_t$  equals the prior and we can sample  $\tilde{o}_t(b)$  using the categorical distribution over the probability vector  $[e_{\tilde{h}_t(b)\tilde{x}_t i}]_i$ . By construction, the comonotonic copula will obey pathwise monotonicity and hence, will ensure that in the counterfactual world, patient does not die before period  $T$ , i.e.,  $H_{T-1} \neq 7$  w.p. 1.